Escola de Camins
Escola Tècnica Superior d'Enginyeria de Camins, Canals i Ports
UPC BARCELONATECH

Multiscale Materials Modelling using DFT-based Localization Relationships

MASTER FINAL THESIS

Final Thesis developed by:
Bhadauria, Anshuman Singh

Directed by:
Saracibar, Carlos Agelet

Master in:
Numerical Methods in Engineering

Barcelona, 28.9.2016

Department of Civil and Environmental Engineering

UPC Barcelona
School of Civil Engineering

Multiscale Materials Modelling using DFT-based Localization Relationships

Anshuman Singh Bhadauria

Submitted in part fulfilment of the requirements
for the degree of Masters in Science

I hereby declare that this thesis and the work reported herein was composed by and originated entirely from me. Information derived from the published and unpublished work of others has been acknowledged in the text and references are given in the list of sources.

Anshuman Singh Bhadauria (2016)

Acknowledgements

I would like to express my deep gratitude to my master thesis director, Prof. Carlos A. Saracibar for the tremendous opportunities he gave me. These opportunities gave me a lot of exposure and a new direction to my life. I am grateful for his patience during the long discussions on the project, and reviewing my work over and over again. His guidance and motivation kept me going during the research for the ICMEg project and writing of this master thesis.

My sincere thanks also goes to Prof. Surya Kalidindi of George. W. Woodruff School of Mechanical Engineering at Georgia Tech, for giving me access to his valuable research and guided me into this new domain of knowledge.

I would also like to thank Prof. Antonia and Lelia for constant support throughout the period of master degree at UPC Barcelona.

Abstract

Multiscale modelling is the need of the hour, and this can be confirmed from the fact that several initiatives have been taken to bring together researchers from different domains by formation of projects like Integrated Computational Materials Engineering (ICME), Materials Genome Initiative etc. This increasing interest can be pertained to the fact that there is a need for creating new materials with desired effective properties for new applications like Additive Manufacturing (AM). Until recently the discovery of new materials was based on empirical methods of trial and error, which takes roughly twenty years to bring in a new material into manufacturing.

Therefore, it is important to address these two difficult problems. First is Multiscale modelling, which enables communication between constitutive models at different length scales, thus improving accuracy of failure predictions and second, is Accelerated Material Discovery, which can reduce the development time of new materials with desired properties.

As it turns out, both these problems are closely related and can be addressed simultaneously. The key to success in both these areas is making problem solving data driven, i.e., converting these non-trivial problems Big Data friendly so that the techniques from Data Science can be used for building scalable, robust and computationally efficient solutions. Another good reason to use data science for these problems is that it makes data reusable i.e., data that was produced during solution of one problem can be used in solving another problem by establishing syntactic material databases, where not only effective properties but also the internal structure of the materials is readily available.

In this thesis, one such mathematical framework called Material Knowledge Systems (MKS) is used to solve both the above mentioned problems. MKS is derived from the Statistical Continuum theories, and has been successfully implemented in real world problems. MKS is based on the rigorous mathematical framework called Material Sensitive Design (MSD), which is further derived from generalized homogenization theories. MSD provides a rigorous methodology for quantification of the internal structure of the material, which spans multiple length and time scales with a *microstructure function*. But the biggest achievement of MSD is that it allows us to incorporate the *n-point* spatial correlations in the homogenization theories. Also it addresses the problem of localization, which has been under addressed as compared to the homogenization problems.

The use of *n-point* spatial correlations to represent the internal structure of the material is

very rigorous, thus, the amount of structural information is substantially large. To deal with this increased amount of information, dimensional reduction techniques like *Principal Component Analysis*, *Naive Bayes* etc., from the field of Data Science. Using these techniques, the material designer can not only visualize the structure-property linkages, but can also begin to solve the inverse problem of creating microstructures using hybrid processes which exhibit the desired effective properties. These linkages are also called *Property-Structure-Process* (PSP) relations. Establishment of such PSP linkages will change the way how materials are created in the future.

I would like to dedicate this thesis to my mother, father, and brother who have supported me unconditionally throughout my life.

Contents

List of Figures

Chapter 1

Introduction

The word "Multiscale" naturally occurs together with materials in nature. The complete description of a material thus needs description of unique attributes at each length scale. The set of these unique attributes at a perceivable small scale are called microstructures. The microstructure of a material can be interpreted as the fingerprint of a material, only difference being that different microstructures can be obtained for the same material by following different heat treatment process or by using a different order of processes. These variations in the microstructures ultimately result in the variation in effective properties of materials. Therefore, it is important for the designer to be aware of the what heat treatment has been used in the production of the material.

This process of material selection can be improved if the designer has access to microstructure information of the material and not just effective properties. However, the amount of information associated with microstructures is very large and to extract "knowledge" out of these huge datasets, some sort of dimension reduction is necessary. With dimension reduction, the vast unwieldy data becomes usable information. However, this information in itself has limited usefulness. In order to make it more useful, the microstructure information has to be related to the effective properties for that microstructure. Such relations are better known *Property-Structure* relations.

With this kind of low dimensional representation of property-structure linkages, it can become easier for designers to choose a set of properties, as it will be clear what kind of microstructure

will produce these properties. At this point, there is a natural desire to understand what processes have to be done to get this desired microstructure? This can be done by establishing the second linkage between *Structure-Process*, i.e., by identifying an ordered set of processes that will produce the desired microstructure. This complete chain is referred to as *Property-Structure-Process*[4] linkages.

In order to establish such linkages it is first essential to find an efficient way of quantifying the morphology or the internal structure of the microstructure. Niezgoda [8] formulated a methodology to rigorously quantify the morphology by treating the microstructure as a set of stochastic rules, controlling the spatial placement of structural attributes, meaning that, each microstructure can be treated as one of the realization of the microstructure process. This allows for comparison between different different microstructures in a statistical way.

n-Point spatial correlations have been used successfully for spatial correlations in many cases[references]. For this thesis, we will use 1-point and 2-point correlations as a means of capturing structure information. Kroner[6, 5] said that effective properties of material can be expressed in terms of a series sum, and the structural information obtained through spatial correlations can be explicitly entered in these terms. A good property of *n-point* relations in that they can also rigorously account for local neighborhoods. Further, it is known that local neighborhoods affect the local response field variable. This amalgamation of spatial correlations of the structure and statistical continuum theory naturally leads to establishment of *PSP* linkages.

Multiscale problems can be classified in two broad categories, first being hierarchical and second concurrent. In hierarchical approach of multiscale modelling, constitutive models are solved at different length scales are solved one after another, transferring information from one model to another whereas, in concurrent method the models at disparate lengths are solved simultaneously while continuously exchanging information between the constitutive models. As one might feel intuitively, true multiscale concurrent simulations are computationally very expensive, and before coming into commercial practice, issues like exascale computing, reduction of data transfer, development of physicality based models need to be addressed. On the other hand, hierarchical methods are computationally more efficient but on the expense

of accuracy, due to simplifying assumptions about the materials. Hierarchical modelling is essentially transferring information from one model to another, and currently this can be thought of as transferring information from one tool to another. The issue of effective communication between different simulation tools is another paradigm of ICME[1, 9] and is formally called Interoperability. Broadly speaking, interoperability can be defined as a standard of ontology, which can be used to describe problem metadata. A complete coverage of interoperability is beyond the scope of this thesis, for a better overview the reader can refer to [9].

In recent years, Finite Element methods have proven to be highly versatile in working with complex geometries, physics and boundary conditions, thus making a strong candidate for localization analysis in multiscale problems. However, in a multiscale scenario in order to include the simulations capturing governing physics of the lower scale, it would require very large meshes, with large amount of data movement leaving the process computationally unviable in real world engineering simulations. Thus MSD emerged as a promising alternative to solve the localization problem.

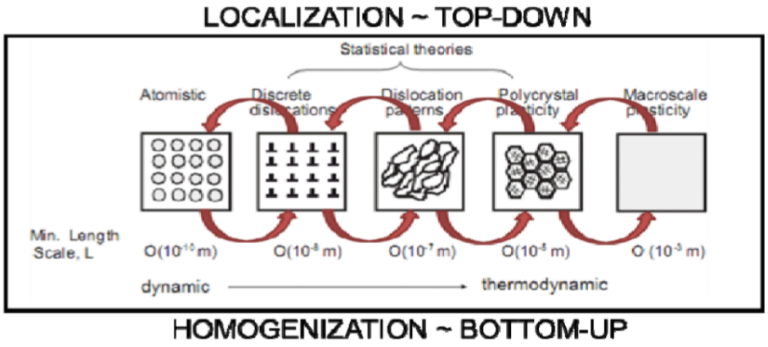

Figure 1.1: Multiscale modelling depends upon effective communication between constitutive relations at different length scales. When the information flown from the micro scale to macro scale, the process is called homogenization and when the flow of information is from macroscale to the microscale it's called localization. Figure courtesy [2]

The generalized homogenization theories to date account for material internal structure by using perturabation theory and Green's function. In this approach a series expansion for localization and homogenization is obtained, with individual terms of the series are convoluted integrals based on Green's function. Microstructure Sensitive Design (MSD) developed by Adams and co-workers [3] is a mathematical framework which was introduced to specifically

enable *Structure-Property* linkages in material systems and addressing the hierarchical multi-scale problems using a microstructure function. MSD enables decomposition of second-order homogenization theories into a physics-dependent function and a microstructure dependent function. This allows for inclusion of *n-Point* spatial correlations in the terms of the effective property series expansions.

In the context of this thesis, we will use the microstructure function [3] to build 1-point and 2-point correlations instead of n-Points in deriving the spectral representation of homogenization theories. The 1-point probability distributions, gives the probability of finding a local state $\mathbf{h}$ at spatial point x in the microstructure. Whereas 2-point spatial correlations denote the probability density of finding local states $\mathbf{h}$ and $\mathbf{h}^{'}$ at spatial position $x + r$, where $\mathbf{r}$ is a random vector in the microstructure.

Materials Knowledge System (MKS) is a computational framework used for extracting 'knowledge' from material systems and establishing PSP linkages. The extraction of linkages are established using classification techniques from the field of Data Science. To make this process of knowledge extraction scalable and computationally efficient MKS discretizes the homogenization theories and statistical descriptions of microstructures using DFT. This results in highly efficient homogenization and Localization models, which can scale to very big microstructure datasets.

1.1 Aim of the thesis

This thesis aims to implement Material Knowledge System (MKS), a computational framework based on the rigorous mathematical framework MSD.

First the theoretical background of MKS and MSD is explained, whose literature was developed by Prof. B.L.Adams [ref], Prof. Surya R. Kalidindi[], and their PhD students Stephen Niezgoda[**?**], Anthony Fast [**?**], Giacomo Landi[7], Massimiliano Binci[**?**].

After the theoretical background, the MKS framework is implemented for a two phase composite material using Python, while the FE simulation for calibration of influence coefficients is done in Abaqus Standard/Explicit.

1.2 Layout of the thesis

- **Chapter** 2 covers the background of probability theory, stochatic processes, Discrete Fourier Transforms (DFT) and Conditional Probability. These concepts will be used in the Chap.(3) to develop a quantitative description of the microstructure.

- **Chapter** 3 provides the detailed description of concepts like local states, local spaces, Discrete Fourier representation of probability density functions, the microstructure function, statistics of microstructure function, n-Point correlation functions, 2-point correlation functions which are the building blocks of MKS.

- **Chapter** 4 describes the generalized homogenization first- and second- order theories.

- **Chapter** 5 covers in detail the core of MSD framework i.e., derivations are done for spectral representations of second-order homogenization theory, followed by explanation of concept of microstructure hull and property closures.

- **Chapter** 6 introduces the localization relationships in the MKS framework and then provides an implementation example of the framework

- **Chapter** 7 provides the conclusions drawn from the work presented and suggestions for future work.

References

[1] John Allison, Dan Backman, and Leo Christodoulou. Integrated computational materials engineering: a new paradigm for the global materials profession. *JOM*, 58(11):25–27, 2006.

[2] Anthony Nathan Fast. *Developing Higher-Order Materials Knowledge Systems*. PhD thesis, Drexel University, 2011.

[3] David T. Fullwood, Stephen R. Niezgoda, Brent L. Adams, and Surya R. Kalidindi. Microstructure sensitive design for performance optimization. *Progress in Materials Science*, 55(6):522–524, 2010.

[4] Surya R Kalidindi. *Hierarchical Materials Informatics: Novel Analytics for Materials Data*. Elsevier, 2015.

[5] E Kröner. Statistical modelling. In *Modelling small deformations of polycrystals*, pages 229–291. Springer, 1986.

[6] Ekkehart Kröner. *Statistical continuum mechanics*. Springer, 1972.

[7] Giacomo Landi, Stephen R. Niezgoda, and Surya R. Kalidindi. Multi-scale modeling of elastic response of three-dimensional voxel-based microstructure datasets using novel dft-based knowledge systems. *Acta Materialia*, 58(7):2716–2725, 2010.

[8] Stephen Richard Niezgoda. *Stochastic representation of microstructure via higher-order statistics: theory and application*. 2010.

[9] Georg J Schmitz and Ulrich Prahl. *Integrative computational materials engineering: Concepts and applications of a modular simulation platform*. John Wiley & Sons, 2012.

Chapter 2

Background

2.1 Microstructure

Microstructure refers to the internal features in heterogeneous materials across many disparate length scales. Inherently, the internal structure of materials are hierarchical in nature. At the macro scale, the material can be seen as partitioned into regions of nearly continuous composition, phase or properties such as grains, fibers or precipitates. A look into the micro scales reveal information about the atomic structure of these partitions, such as lattice constants or lattice orientations of the crystalline components.Further magnification reveals the defects in the atomic structure of the constituent phases including the state of vacancy or interstitial concentrations, the presence of fine scale precipitates, voids, grain boundaries, and the state of dislocation in the material [2, 3]. Further magnification reveals the electronic and quantum states of the atoms and their aggregates.

It is essential to understand how local properties of a material depend upon the statistical distributions of a small set of local state parameters. Of particular importance, is to understand how the spatial distributions of microstructural features impact the properties and performance of a material.

Historically, the description of microstructure focused only on the first-order descriptors, often referred to as 1-point statistics. However, in recent years, higher-order statistical descriptors of microstructure continue to be developed, which aim to capture the main topological features

such as clustering, periodicity, connectivity, the fractal nature of structure etc.

The next section reviews some concepts of probability theory and stochastic processes, which are used in describing n-point correlations which naturally lead to effective property homogenization schemes by representing the microstructure as a random process.

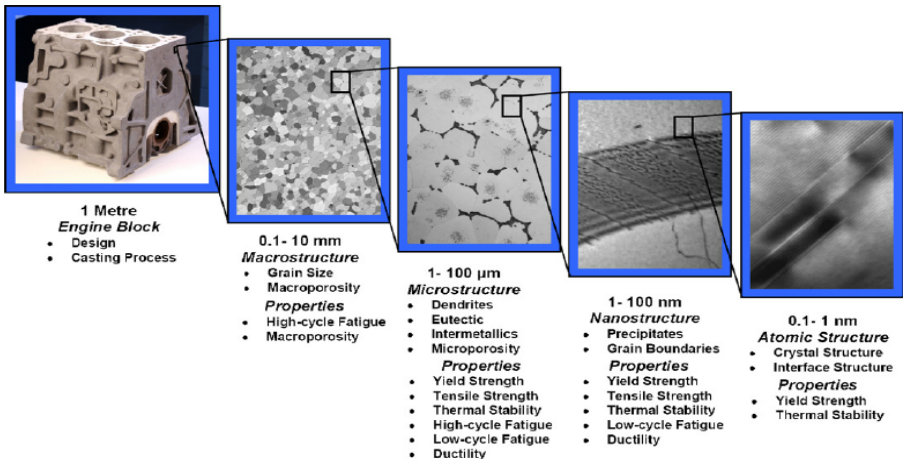

Figure 2.1: Hierarchy of metallurgical length scales that influence the property balance. Image courtesy [1]

2.2 Review of Probability Theory and Stochastic Processes

The probability space is described by the ordered triplet $(\Omega, \mathcal{F}, \mathcal{P})$. The first element Ω is a non-empty set with elements ω. Each element, ω, is an experimental outcome and the set Ω is called the sample space. $\mathcal{F}$ is the set of all possible events and is formally defined as a Borel σ-algebra for which the following axioms must hold:

$$\begin{aligned} \Omega &\in \mathcal{F} \\ If \quad \mathcal{A} \in \mathcal{F} \quad then \quad A^c &\in \mathcal{F} \\ If \quad A, B \in \mathcal{F} \quad then \quad A \cup B &\in \mathcal{F} \end{aligned} \tag{2.1}$$

where A^c denotes the compliment to set A. $\mathcal{P}$ denotes the probability measure of $\mathcal{F}$.

2.2.1 Random variables

Given a probability space defined by the ordered triplet $(\Omega, \mathcal{F}, \mathcal{P})$, to every experimental outcome ω we can assign a number $\mathbf{x}(\omega)$.In doing so, we define a function $\mathbf{x}$ with a domain Ω and a range. This function is termed a random variable if it satisfies the following conditions:

$$\text{The set } \mathbf{x} \leq x \text{ is an event for every } x. \tag{2.2}$$

$$\mathcal{P}\{\mathbf{x} = \infty\} = 0 \quad \mathcal{P}\{\mathbf{x} = -\infty\} = 0 \tag{2.3}$$

where $\{\mathbf{x} \leq x\}$ is the subset of Ω consisting of all experimental outcomes such that $\{\mathbf{x}(\omega) \leq x\}$. This means, a random variable $\mathbf{x}$ assigns a number $\mathbf{x}(\omega)$ to every outcome ω.

The probability $\mathcal{P}\{\mathbf{x} \leq x$ is the cumulative distribution function (CDF), represented by $F_x(x)$ of the the random variable $\mathbf{x}$ and is defined over the domain $-\infty<x<\infty$. $F_x(x)$ is a non-decreasing function of x which takes the values $F(-\infty) = 0$ and $F(\infty) = 1$. The better known probability density function (PDF) is defined as the derivative of the CDF:

$$f_x(x) = \frac{dF_x(x)}{dx} \tag{2.4}$$

The expected value or mean of a random variable is given by:

$$E\{\mathbf{x}\} = \int_{-\infty}^{\infty} x f(x) dx \tag{2.5}$$

For a random variable with mean μ the quantity $\mathbf{x} - \mu$ represents the deviation of the random variable from its mean. The variance of a random variable is the average square deviation of $\mathbf{x}$ about μ

$$\sigma^2(\mathbf{x}) = E\{(\mathbf{x} - \mu)^2\} = \int_{-\infty}^{\infty} (x - \mu)^2 f(x) dx > 0. \tag{2.6}$$

Higher order moments can be defined as

$$\mathcal{M}_n = E\{\mathbf{x}^n\} = \int_{-\infty}^{\infty} x^n f(x) dx \tag{2.7}$$

where n is an integer referred to as the order.

A random vector (or a random field) is a vector $\mathbf{X} = [\mathbf{x}_1, ...\mathbf{x}_n]$ whose components are random variables with joint CDF $F(X) = F(x_1, ...x_n) = \mathcal{P}\{\mathbf{x}_1 \leq x_1, ...\mathbf{x}_n \leq x_n\}$. The joint PDF is defined as

$$f(X) = f(x_1, ...x_n) = \frac{\partial^n F(x_1, ..., x_n)}{\partial x_1, ..., \partial x_n} \tag{2.8}$$

The correlation matrix of the random vector $\mathbf{X}$ is defined as

$$R_{ij} = E\{\mathbf{x}_i \mathbf{x}_j\} = E\{\mathbf{X}\mathbf{X}^T\} \tag{2.9}$$

and by extension the covariance matrix as

$$C_{ij} = R_{ij} - \mu_i \mu_j \tag{2.10}$$

Two random variables $\mathbf{x}_1$ and $\mathbf{x}_2$ are independent if $F(x_1, x_2) = F_{x1}(x1)F_{x2}(x2)$ and $f(x_1, x_2) = f_{x1}(x1)f_{x2}(x2)$. Two random variables are considered orthogonal if $E\{\mathbf{x}_1\mathbf{x}_2\} = 0$. A random vector of orthogonal components must have a diagonal correlation matrix.

2.2.2 Stochastic Processes

Building upon the previous section, a stochastic process $\mathbf{x}(t)$ is, by extension, a set of rules that assign a function $x(t, \omega)$ to every experimental outcome ω of the experiment Ω. Stochastic processes are largely concerned with time-series, thus the variable t is defined over the domain of real numbers,$\mathbb{R}$, for a continuous time process or the integers, $\mathbb{Z}$, for a discrete time process.

In context of microstructures, we consider an ensemble of functions (micrographs or 3D datasets), a realization or an instantiation of the random process. Information about the Microstructure is obtained by an ensemble average over the individual instantiations.

When x(t) is interpreted as a rule for assigning a function to an experimental outcome, these rules take form of a set of associated probability distributions. This lets us partially quantify the microstructure (random process) using first or second order statistical descriptors. The

mean $\mu(t)$ of the process $\mathbf{x}(t)$ is the expected value of the random variable $\mathbf{x}(t)$

$$\mu(t) = E\{\mathbf{x}(t)\} = \int_{-\infty}^{\infty} x f(x,t) dx \tag{2.11}$$

and the autocorrelation is defined as

$$R(t_1, t_2) = E\{\mathbf{x}(t_1)\mathbf{x}(t_2)\} \int_{-\infty}^{\infty} \int_{-\infty}^{\infty} x_1 x_2 f(x_1, x_2; t_1, t_2) dx_1 dx_2 \tag{2.12}$$

As in Eq.(2.10) the autocovariance of a stochastic process is defined

$$C(t_1, t_2) = R(t_1, t_2) - \mu(t_1)\mu(t_2) \tag{2.13}$$

A process is considered to be wide-sense stationary if it has a constant mean

$$E\{\mathbf{x}(t)\} = \mu \tag{2.14}$$

and its autocorrelation depends only on $\tau = t_1 - t_2$

$$E\{\mathbf{x}(t+\tau)\mathbf{x}(t)\} = R(\tau) \tag{2.15}$$

Most statistical parameters of interest can be expressed in terms of expected values of some functional of the random process $\mathbf{x}(t)$. The point estimate of a parameter is a function, $\hat{\theta} = g(X)$, of an observation vector $X = [x_1, ..., x_n]$.$\hat{\theta}$ is considered an unbiased estimator of the parameter θ if $E\{\hat{\theta}\} = \theta$. $\hat{\theta}$ is termed a consistent estimator of θ if the function $g(X)$ can be chosen such that the estimation error $|\hat{\theta} - \theta| \to 0$ as $n \to \infty$.

2.2.3 Conditional Probability and Bayes Theorem

Conditional probabilities describe the likelihood of some event A occurring given that event B has already occurred. The conditional probability is defined as

$$\mathcal{P}(A|B) = \frac{\mathcal{P}(A \cap B)}{\mathcal{P}(B)} \tag{2.16}$$

Two random events are considered statistically independent iff

$$\mathcal{P}(A \cap B) = \mathcal{P}(A)\mathcal{P}(B) \tag{2.17}$$

For two independent events, this can also be written as

$$\mathcal{P}(A|B) = \mathcal{P}(A) \tag{2.18}$$

The relationship between $\mathcal{P}(A|B)$ and $\mathcal{P}(B|A)$ is given by Bayes' theorem as

$$\mathcal{P}(B|A) = \frac{\mathcal{P}(A|B)\mathcal{P}(B)}{\mathcal{P}(A)} \tag{2.19}$$

Using Bayes' theorem we can update our expectations of experimental outcomes based on additional observed data. $\mathcal{P}(B)$ is referred to as the prior probability of B, because it does not take event A into account. $\mathcal{P}(A|B)$ is referred to as the likelihood. Additionally $\mathcal{P}(A)$ is often called the marginal probability and acts as a normalizing constant.

For two continuous random variables $\mathbf{a}$ and $\mathbf{b}$ the likelihood function can be written as

$$L(\mathbf{a}|\mathbf{b}) = f(\mathbf{a}|\mathbf{b} = b) \tag{2.20}$$

and the posterior probability density of b, i.e. the conditional probability distribution of b given the observed data a can be written as

$$f(\mathbf{b} = b|\mathbf{a}) = constant.L(\mathbf{a}|\mathbf{b})f(\mathbf{a}) \tag{2.21}$$

2.3 Discrete Fourier Transforms

Spectral (Fourier) representations not only provide compact representation of functions, but also facilitates efficient computations of the microstructure-property relations.

Using the Fourier series any arbitrary function can be decomposed as

$$g(x) = \sum_{n=0}^{\infty} a_n \theta_n(x) \tag{2.22}$$

and the corresponding Fourier coefficients a_n can be found as

$$a_n = \frac{1}{c_n} \int_R g(x)\theta_n(x)w(x)dx \tag{2.23}$$

Where $\theta_n(x) = e^{\frac{2\pi inx}{N}}$ and $R = [a, a + N]$ represent the traditional complex Fourier series for a function with period N.

DFTs prove useful in the context of microstructure quantification because usually microstructure data in not available as a continuous analytic function but, rather, as a discrete set of sample points. In such cases, representation of data in terms of DFT proves beneficial in terms of computational advantage. Here DFT is just the discrete analog of the complex Fourier series.

Any arbitrary distribution function $f(x)$ defined on some interval $[0, X]$, sampled at N equally spaced points labeled $[0, 1, ..., N - 1]$ can be approximated from the samples as

$$f(x) \approx f_n \mathcal{X}_n(x) \tag{2.24}$$

$$\mathcal{X}_n(x) = \begin{cases} 1 & \text{if} x \in [0, 1, \ldots, N-1] \\ 0 & \text{otherwise} \end{cases}$$

The DFT of $f(x)$ can be written as

$$f_n = \frac{1}{N} \sum_{k=0}^{N-1} F_k e^{2\pi i \frac{nk}{N}} \tag{2.25}$$

where Fourier coefficients can be given by

$$F_k = \sum_{n=0}^{N-1} F_k e^{-2\pi i \frac{nk}{N}} \tag{2.26}$$

The use of the DFT, rather than generalized Fourier series for aperiodic functions such as Chebychev or Legendre series, is because of the availability of efficient fast Fourier transform (FFT) algorithms. As written Eq. (2.28) requires N^2 operations, which reduces to $\mathcal{O}(NlogN)$ using FFT algorithms which results in computational efficiency.

Some DFT properties that will prove useful in decomposition of signals in the later chapter are described very briefly next, for details any text on Digital Signal Processing can be referred.

1. The first DFT property is Plancherel's theorem, which relates an inner product in real space to an inner product in Fourier space. It states

$$\sum_{n=0}^{N-1} f_n . g_n^* = \frac{1}{N} \sum_{k=0} F_k . G_k^* \tag{2.27}$$

   where (.) operator indicates inner product and ()* indicates complex conjugate.

2. A special case of Plancheral's theorem is Parseval's theorem, which states that the total energy of a function in real space is equal to the total energy of the Fourier transform:

$$\sum_{n=0}^{N-1} |f_n|^2 = \frac{1}{N} \sum_{k=0}^{N-1} |F_k|^2 \tag{2.28}$$

3. Next is the convolution theorem, which states that convolution in the real space is equivalent to multiplication in the Fourier space or

$$(f * g)_m = \sum_{n=0}^{N-1} f_n g_{n-m} = \Im^{-1}(F_k . G_k)_m \tag{2.29}$$

   where $\Im^{-1}$ indicated the inverse DFT

2.4 Principal Component Analysis

Principal component analysis (PCA)[] or proper orthogonal decomposition is used for lower dimensional, or reduced order, representations of complex microstructure datasets and their associated higher-order probability distributions.

PCA basically projects a high-dimensional data set into a new orthogonal coordinate frame where the axes are defined by the directions of highest variance. The first axis of data, or the first principal component is the direction of highest variance in the data, the second principal coordinate is the direction of highest variance orthogonal to the first axis. A more detailed technical background of PCA can be found in any machine learning textbo.

For the purpose of thesis the basic algorithm will be explained. Taking an ensemble of L vectors of distributions, the PCA decomposition of the l^{th} member, f^l, of the ensemble can be written as

$$f^l = \sum_{j=1}^{L-1} \alpha_j^l \phi_j + \bar{f} \tag{2.30}$$

where $\bar{f}$ represents the mean vector. In Eq.(2.32),ϕ_j represents the orthogonal basis set (i.e. the principal directions) and α_j^l represents the corresponding weights of the l^{th} member.

The steps of PCA decomposition can be written as

1. Mean center the data. $\Phi^l = f^l - (\bar{f})$
2. Calculate the co-variance matrix of the data. $C = \frac{1}{L} \sum_L \Phi^l (\Phi^l)^T$
3. Perform the eigenvalue decomposition. $C\phi_j = b_j \phi_j$
4. Project mean centered data into the eigenspace to fiend the weights. $\alpha_j^l = (\phi_j)^T \Phi^l$

References

[1] CJ Bettles, MA Gibson, and Su-Ming Zhu. Microstructure and mechanical behaviour of an elevated temperature mg-rare earth based alloy. *Materials Science and Engineering: A*, 505(1):6–12, 2009.

[2] Surya R Kalidindi. *Hierarchical Materials Informatics: Novel Analytics for Materials Data*. Elsevier, 2015.

[3] Stephen Richard Niezgoda. *Stochastic representation of microstructure via higher-order statistics: theory and application*. 2010.

Chapter 3

Microstructure Representation

3.1 Introduction

Microstructure contain very large amount of information in a very tightly packed space. However, in order to understand the effects of localization, it is essetial to be quantify this information in a meaningful way. In this regard, Niezgoda [9] presented a mathematical framework for quantifying the material structure stochastically using the spatial correlation of the microstructure. It is worth noting that spatial correlations can be found using either lineal path functions, or radial distribution functions or n-point correlations. However, *n-point* spatial correlations have proved to cover structural information most exhaustively [3].

Spatial correlations can be, the 1-point statistics, which give the probability of finding a local state of interest at a random point in the structure or they can be 2-point statistics, which capture the joint probability of finding specified local states h and $h^{'}$ at the head and tail of randomly placed vector in the microstructure. This concept can further extended to *n-Point* correlations.

An added advantage of using a stochastic process like n-points is that, it also allows the quantification of variance associated with the structure. However, due to the increased amount of structural information in the 2-point statistics, there are many redundancies [8]. This problem is however resolved by using dimensionality reduction techniques such as PCA [10]. The details of the microstructure quantification process using n-point statistics based on microstructure

function and local sates are discussed next. The DFT-based digital representation of local distribution function, microstructure function and spatial correlations are presented.

3.2 Local State and Local State Space

The local state of interest, denoted by **h**, in a particular material system are those attributes that depend on spatial position and affect the local properties of that position. Local states can be a combination of the phase, composition, lattice orientation or other local descriptors. If for example, the microstructure of interest comprises of two distinct thermodynamic phases and considering only volume fraction as an attribute is considered as an attribute. Let's call the two local states "white" and "black" for simplicity, then the first order local state space could be described by the set, $H = \{black, white\}$. Further, the second order local state space can be described as $H = \{(white, white), (white, black), (black, white), (black, black)\}$ as seen in the Fig. (3.1). A more realistic example of local states can be seen in Fig.(3.2), taken from a micrograph of a Ti-Mn alloy. An important note here is that, local state space has all the local states possible in a material, whether or not they are present in the microstructure sample.

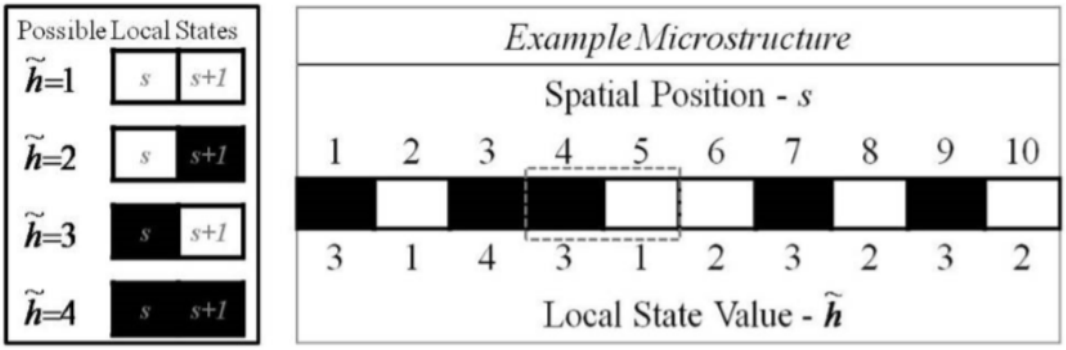

Figure 3.1: A simplified one dimensional microstructure with two phases (black and white):(Right): and the complete local state space, showing all possible second order local states (Left). The redundancies in information captured by higher order statistics can be seen for the description of local state in spatial cell 4, where the local state assigned for spatial cell 3 and spatial cell 4 essentially are giving the same information about spatial cell 4.Figure courtesy[4]

Now to generalize this concept, let $\mathbf{x}$ denote a material point such that $\mathbf{x} \in \Omega$. $\mathbf{x}$ can be associated with one or more local states $\mathbf{h} \in H$ (in the immediate neighborhood of $\mathbf{x}$). Here, H represents the complete set of distinct local states that could theoretically be found across the

length scales of interest.

For example, amongst the elastic properties of a single-phase polycrystal, the important microstructure parameters are thermodynamic phase, ρ, and crystallographic orientation, g, as depicted in Fig. 2.2. H is represented as the ordered pair $h = (\rho, g)$ and local state space, H, is formally defined as

$$H = \left\{ (\rho, g) | (\rho, g) \in \bigcup_{\rho} H_\rho, H_\rho = \{(\rho, g) | g \in FZ(\rho)\} \right\} \tag{3.1}$$

where $FZ(\rho)$ denotes the fundamental zone of ρ or the set of physically-distinct lattice orientations for the crystal symmetry of ρ.

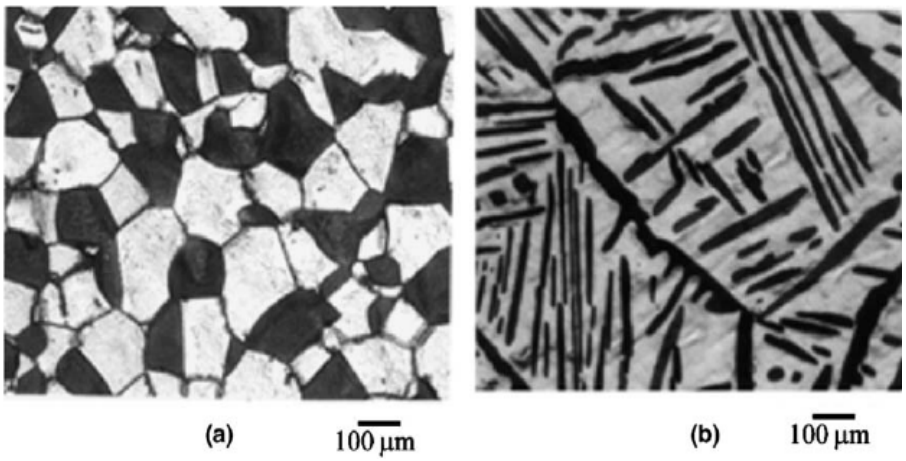

Figure 3.2: Micrographs demonstrating the concept of local state showing a two phase Ti-Mn alloy: phases(left) and crystallographic orientations (right).Image courtesy (Ankem et. al, 2006)[1]

Now, if the local state h, found at position x, in a material sample is considered as a random variable $h(x)$, we can define a local state distribution $f(h)$ over the local state space as:

$$f(h)dh = \frac{V_{h \pm \frac{dh}{2}}}{V} \tag{3.2}$$

where $\frac{V_{h \pm \frac{dh}{2}}}{V}$ denotes volume fraction of the microstructure that are associated with local states lying within an invariant measure dh of local state h. Also, by definition, if the local state

distribution function $f(h)$ is integrated over the entire local state space H,

$$\int_H f(h)dh = 1 \tag{3.3}$$

When considering only the orientations characteristics of single-phase polycrystals, the local state distribution function is called Orientation Distribution Function (ODF).

3.3 Microstructure Function

For effective statistical representation of microstructure, Adams and co-authors [6] introduced the microstructure function, $m(h, x)$. A slightly different definition of the microstructure was proposed by Niezgoda, in terms of a stochastic process [10].

In order to arrive at a formal definition of microstructure function. The complete set of material points is represented by Ω. Now, the microstructure function can be defined as the rules that assigns a function (local state field), $m(x, h)$, to every microstructure realization. A visual representation of the the microstructure function can be seen in Fig.(3.3)

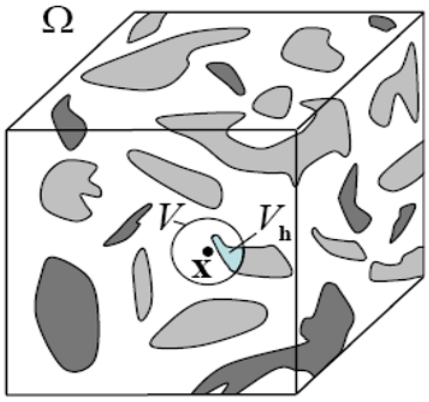

Figure 3.3: Schematic representations of microstructure function courtesy Binci M.[2].

Now the microstructure function $m(x, h)$, which represents the probability density of finding a local state **h** at a spatial point x is formally defined as

$$m(x, h)dh = \frac{dV}{V}|_{x,h} \tag{3.4}$$

where $\frac{dV}{V}$ indicates the volume fraction of material with associated local state within a neighborhood element dh about h, in a neighborhood of volume V surrounding point x.

Normalizing Eq.(3.1) by volume of the realization ω

$$\frac{1}{vol(\omega)} \int_{x \in \omega} \int_{h \in H} m(x, h, \omega) dh dx = 1 \tag{3.5}$$

For practical purposes, microstructure is discretized as shown in Fig.(3.4) on a grid. This discrete description of the microstructure function is a more natural reflection of the available information, as most experiments typical produce discretized information in form of datasets. For instance, microstructure functions $m^1_{(1,2)} = 1, m^2_{(1,2)} = 0$ can be interpreted as, the volume fraction of *white phase* in spatial cell (1,2) is 1, where as the volume fraction of *grey phase* in spatial cell (1,2) is 0. Now to generalize, let the local state space H be binned into N discrete local states labeled $n = 1, 2, \ldots, N$ and let the spatial domain $x \in \Omega$ be binned into a uniform grid of S cells, whose nodes are enumerated by the index s with $s = 0$ corresponding to the zero vector. Then, $m(x, h)$ can be discretized as m^n_s. The following properties follow from Eqs. (3.6) and (3.7)

$$\sum_{n-1}^{N} m^n_s = 1, \qquad 0 \leq m^n_s, \qquad \sum_{s=0}^{S-1} m^n_s = V^n S \tag{3.6}$$

where V^n denotes the volume fraction of local state n in the microstructure.

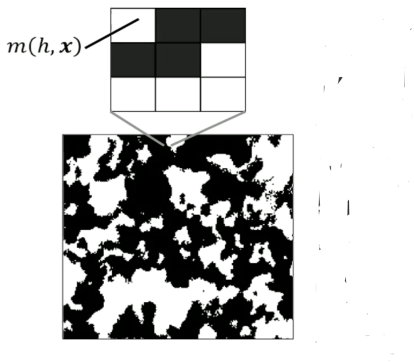

Figure 3.4: Micrograph of a two phase heterogeneous material.

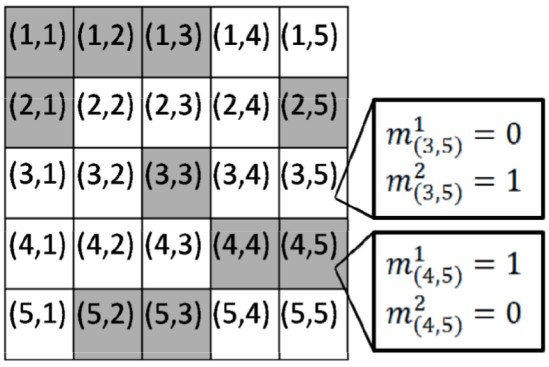

Figure 3.5: Simplified view of the microstructure as a discretized domain. Picture courtesy Landi G. [7]

3.3.1 Spectral representation of microstructure function

The discretized representation of the microstructure function m_S^n can be transformed in a Fourier series using primitive basis functions [5].

$$m(\mathbf{x}, h) \approx \sum_{s=0}^{S_1} \sum_{n=1}^{N} N m_s^n \mathcal{X}_s(\mathbf{x}) \mathcal{X}^n(h) = \sum_{s=0}^{S_1} \sum_{n=1}^{N} D_s^n \mathcal{X}_s(\mathbf{x}) \mathcal{X}^n(h) \tag{3.7}$$

where D_s^n is related to the probability distribution $s_f(h)$ in cell s.

$$D_s^n = \frac{N}{V_s V_n} \int_{\mathbf{x} \in \omega_s} \int_{h \in \omega_n} m(\mathbf{x}, h) dh d\mathbf{x} \tag{3.8}$$

where ω_s and ω_n are cells in real and orientation space of volume V_s and V_n. The Fourier coefficients are called *microstructure coefficients* and are constrained as

$$\sum_{n=1}^{N} D_s^n = N \tag{3.9}$$

3.4 Statistics of Microstructure Function

To completely describe the statistics of microstructure function lets consider a material system where the local state space defined by the combination of k microstructure features of interest, such that $h = (\alpha_1, \ldots, \alpha_k)$. Now, for any material point x, the local state is described by the random vector $\mathbf{h} = [\alpha_\mathbf{1}, \ldots, \alpha_\mathbf{k}]$. The evaluation of the microstructure function $\mathbf{m}(x, h)$, for a specific material point x, is a random vector with CDF

$$F(h, x) = \mathcal{P}\{\mathbf{h}(x) \leq h\} \tag{3.10}$$

where the notation $mathcalP\{\mathbf{h}(x)$ is interpreted as $mathcalP\{\alpha_1(x) \leq \alpha_1, \ldots, \alpha_k(x) \leq \alpha_k\}$. The local state joint PDF at each position x is given as

$$f(h, x) = f(\alpha_1, \ldots, \alpha_k, x) = \frac{\partial F(h, x)}{\partial h} \tag{3.11}$$

From the extension of univariate distributions, the probability that h is in a region $\mathcal{H}$ of the local state space H is given by

$$\mathcal{P}\{\mathbf{h} \in \mathcal{H}\} = \int_{\mathcal{H}} f(\alpha_1, \ldots, \alpha_k) dh\alpha_1 dh\alpha_2 \ldots dh\alpha_k \tag{3.12}$$

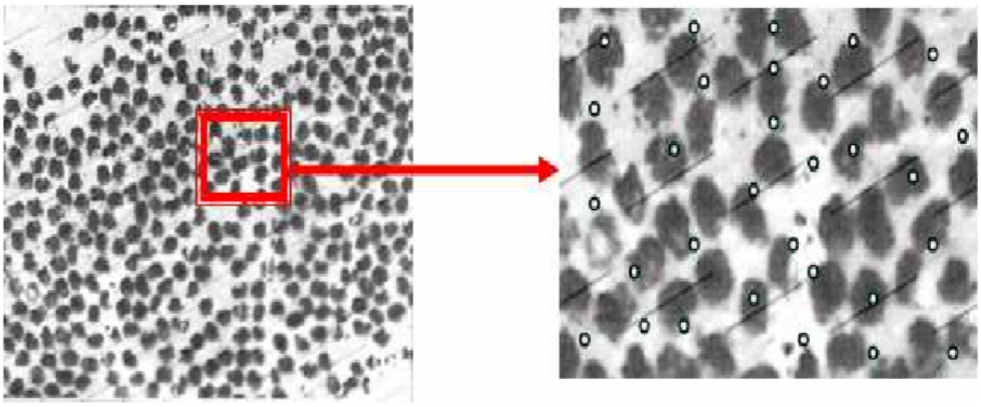

Figure 3.6: Schematic representations of one-point statistics measurement in a two-phase composite microstructure. Image courtesy [11]

Here the PDF $f(h, x)$ is referred to as the first order density or 1-point statistics of the Microstructure, and can be interpreted as the spatially resolved volume fraction of local state $h = (\alpha_1, \alpha_2, \ldots, \alpha_k)$.

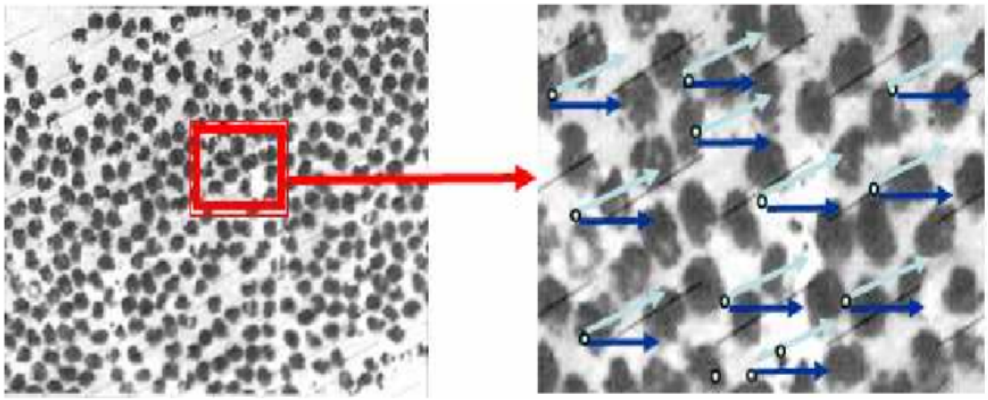

Figure 3.7: Schematic representations of two-point stastistics measurment in a two-phase composite microstructure. Image courtesy [11]

The second-order CDF of $\mathbf{m}(x, h)$ is defined as

$$F(h1, h2; x1, x2) = \mathcal{P}\mathbf{h}(x1) \leq h_1, \mathbf{h}(x2) \leq h_2 \tag{3.13}$$

which is the joint CDF of random vectors $\mathbf{h}(x_1)$ and $\mathbf{h}(x_2)$. The second order PDF or 2-point statistics is then given as

$$f(h_1, h_2; x_1, x_2) = \frac{\partial^2 F(h_1, h_2; x_1, x_2)}{\partial h_1 \partial h_2} \tag{3.14}$$

The 2-point correlations for a particular set of microstructure can be put in form of a NxN array as seen in Fig.(3.8). However, out of the N^2 terms of the correlations matrix, only $(N-1)$ are independent (Niezgoda, et al, 2008).

$$^{np}f_{\mathbf{t}} = \begin{bmatrix} ^{11}f_{\mathbf{t}} & ^{12}f_{\mathbf{t}} & \dots & \dots & ^{1N}f_{\mathbf{t}} \\ ^{21}f_{\mathbf{t}} & \ddots & & & \vdots \\ \vdots & & \ddots & & \vdots \\ \vdots & & & \ddots & \vdots \\ ^{N1}f_{\mathbf{t}} & \dots & \dots & \dots & ^{NN}f_{\mathbf{t}} \end{bmatrix}$$

Figure 3.8: 2-point correlations matrix.

The terms of the diagonal are called *autocorrelations* and the off diagonal terms are called *cross-correlations*. Further Frisch and Stillinger (Refer) showed that for a 2-phase material, only one of the four correlations is independent, i.e., if one of the four correlations is known, the others can be calculated.

3.4.1 Spectral representation of 2-Point spatial correlations

Similar to the spectral representation of microstructure functions, the two point correlations can be represented digitally as

$$f(h,h^{'}|r) \approx \sum_{p}\sum_{n}\sum_{t} f_t^{np}\mathcal{X}_t(r)\mathcal{X}^n(h)\mathcal{X}^p(h^{'}) \tag{3.15}$$

where index t bins the vector space associated to r. 2-point correlations are the statistical measures that contain spatial information. As compared to 1-point statistics the amount of information contained in 2-point statistics is very large. Fortunately there are many redundancies in the 2-point correlations, which can be identified and a low dimensional representation using PCA is possible.

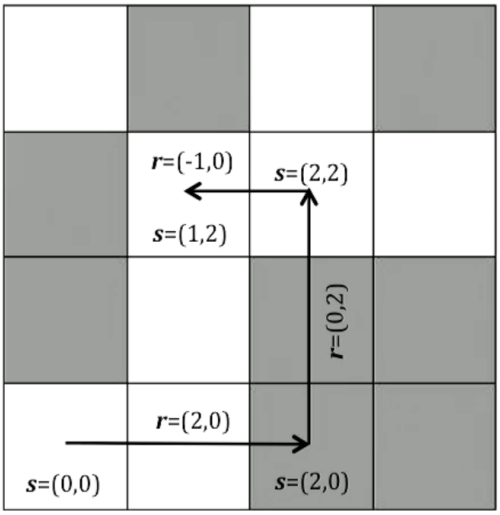

Figure 3.9: 2-point statistics are the conditional probability of finding a local state n at spatial bin s, while simultaneously finding local state p at spatial bin $s+r$.

Now from the previous equation, an expression relating digital representation of microstructure and 2-point statistics can be written as

$$f_t^{np} = \frac{1}{S}\sum_{s=0}^{S-1} m_s^n m_{s+t}^p \tag{3.16}$$

S can be considered the complete space of trials, one bin can be equated to one event. Eq.(3.30)

can also be written as

$$f_j[h, h^{'}; r] = \frac{1}{\Omega_j[r]} \sum_s m_j[h; s] m_j[h^{'}; s + r] \tag{3.17}$$

Using the DFT convolution theorem, the Fourier transform of f_t^{np} can be written as

$$\Im(f_t^{np}) = F_k^{np} = \frac{1}{\mathcal{S}} \Im(m_s^n)^* \Im(m_s^p) \tag{3.18}$$

where (.)*indicates complex conjugation and $\Im(.)$ indicates the DFT. Eq.(3.14) is the most efficient way of calculating 2-point correlation functions (Niezgoda et al). As a result of Eq.(3.31), 2-point statistics computation is reduced to computing discrete Fourier transforms of m_S^n.

3.4.2 Reduced order representation using PCA

Although, 2-point statistics capture extensive and exhaustive representation of microstructure, but as a result of this there is a lot of redundancies in the data. Dimensional reduction techniques create low dimensional microstructure descriptors from the sets of spatial correlations (based on different selections of h and $h^{'}$) with PCA. The PCA dimensionality reduction can be formally described as

$$f_j[l] \approx \sum_{k \in K} \mu_j[k] \phi[k, l] + \bar{f[l]} \tag{3.19}$$

where $f_j[l]$ represents low rank approximation of 2-point statistics, where $f_j[h, h^{'}; r]$, indices from Eq.(3.31) are represented as a vector with single index given by $f_j[l]$ where l is a unique integer for every combination of $h, h^{'}$ and r. The $\mu[k]$ are lower dimensional microstructure descriptors (transformed 2-point statistics) or principal component scores. $\phi[k, l]$ are the calibrated principle components (PCs) and the $\bar{f[l]}$ are mean values from the calibration ensemble of $f_j[l]$ for each l. The $k \in K$ indices refer to the $\mu_j[k]$ in decreasing order of significance and are independent of $l, l^{'}$ and r. Another advantage is that $f_j[l]$ can be reconstructed to sufficient fidelity with only a small subset of $\mu_j[k]$ [8].

References

[1] Sreeramamurthy Ankem, Harold Margolin, Charles A Greene, Brett W Neuberger, and P Gregory Oberson. Mechanical properties of alloys consisting of two ductile phases. *Progress in Materials Science*, 51(5):632–709, 2006.

[2] Massimiliano Binci. *A novel spectral framework for second-order homogenization theories*. PhD thesis, Drexel University, 2008.

[3] Ahmet Cecen, Tony Fast, and Surya R Kalidindi. Versatile algorithms for the computation of 2-point spatial correlations in quantifying material structure. *Integrating Materials and Manufacturing Innovation*, 5(1):1, 2016.

[4] Anthony Nathan Fast. *Developing Higher-Order Materials Knowledge Systems*. PhD thesis, Drexel University, 2011.

[5] Gerald B Folland. *Real analysis: modern techniques and their applications*. John Wiley & Sons, 2013.

[6] David T. Fullwood, Stephen R. Niezgoda, Brent L. Adams, and Surya R. Kalidindi. Microstructure sensitive design for performance optimization. *Progress in Materials Science*, 55(6):522–524, 2010.

[7] Giacomo Landi. *A Novel Spectral Approach to Multi-Scale Modeling*. 2011.

[8] Giacomo Landi, Stephen R. Niezgoda, and Surya R. Kalidindi. Multi-scale modeling of elastic response of three-dimensional voxel-based microstructure datasets using novel dft-based knowledge systems. *Acta Materialia*, 58(7):2716–2725, 2010.

[9] Stephen R Niezgoda, Yuksel C Yabansu, and Surya R Kalidindi. Understanding and visualizing microstructure and microstructure variance as a stochastic process. *Acta Materialia*, 59(16):6387–6400, 2011.

[10] Stephen Richard Niezgoda. *Stochastic representation of microstructure via higher-order statistics: theory and application*. 2010.

[11] Ghazal Peydaye Saheli. Homogenization relations for elastic properties based on two-point statistical functions. 2006.

Chapter 4

Decomposition of Homogenization Theories for inclusion of *n-Point* Statistics

Expressions for effective properties of heterogeneous materials can be derived using statistical continuum theories [6] in terms of bounds or estimates of the elastic properties. The effective properties are represented by a series expansion, whose terms represent the higher order spatial correlations of local states (see Chapter 2). The *bounds* of the effective properties account for 1-point and 2-point statistics of the microstructure and are derived from variational principles. On the other hand, *estimates* of the effective properties are derived from equilibrium equations of an infinite continuous medium subjected to far-field uniform boundary conditions. In the following sections first-order and second-order homogenization theories are reviewed from [2] and the Material Sensitive Design (MSD) framework [3] is discussed.

4.1 First-Order Theory

First-order theories provide effective properties of composite materials in conservative bounds. They are based on variational principles and appear as inequalities in form of strain energy

densities. In the first-order theory, the local strain energy density ω of a composite is given by

$$\omega = \frac{1}{2}\mathbf{C}\epsilon.\epsilon = \frac{1}{2}\mathbf{S}\sigma.\sigma \tag{4.1}$$

where local strain ϵ and stress σ are second-rank stress. The local stiffness $\mathbf{C}$ and compliance $\mathbf{S}$ are symmetric and positive-definite fourth rank tensors. The Voigt-Reuss bounds can be obtained as from the principle of minimum potential and complimentry energy as

$$\frac{1}{2vol(\Omega)}\int_{\Omega}\mathbf{C}\epsilon.\epsilon d\mathbf{x} = \frac{1}{2}\mathbf{C}^{*}\left\langle\epsilon\right\rangle.\left\langle\epsilon\right\rangle \leq \frac{1}{2}\left\langle\mathbf{C}\right\rangle\left\langle\epsilon\right\rangle.\left\langle\epsilon\right\rangle, \tag{4.2}$$

$$\frac{1}{2vol(\Omega)}\int_{\Omega}\mathbf{S}\sigma.\sigma d\mathbf{x} = \frac{1}{2}\mathbf{S}^{*}\left\langle\sigma\right\rangle.\left\langle\sigma\right\rangle \leq \frac{1}{2}\left\langle\mathbf{S}\right\rangle\left\langle\sigma\right\rangle.\left\langle\sigma\right\rangle \tag{4.3}$$

inverting Eq.(5.3) and substituting $\mathbf{C}^{*} = (\mathbf{S}^{*})^{-1}$, the bounds of $\mathbf{C}^{*}$ in a compact notation can be written as

$$\left\langle\mathbf{S}\right\rangle^{-1} \leq \mathbf{C}^{*} \leq \left\langle\mathbf{C}\right\rangle \tag{4.4}$$

The 1-point bounds can't be violated as they are based on energy conservation, and are easy to compute. But in practice, 1-point bounds are impractical as the bounds are usually very far apart.

4.2 Second-Order Theory

Spatial correlations in the form of 2-point statistics can be included in the homogenization theories for prediction of isotropic or anisotropic properties of materials. Second order theories can be broadly classified on basis of the type of formulation used. The first category is based on variational formulation referred to as Hashin-Shtrikman (GHS) bounds [4], whereas the second category uses perturbations of the local stress and strain fields to obtain bounds and estimates of the effective properties [7]. A summary of expressions of both categories is presented next.

4.2.1 Hashin-Shtrikman Bounds

[1] formulated the second-order GHS bounds for the effective elastic stiffness tensor, $\mathbf{C}^*$ as,

$$\mathbf{C}^l + \mathbf{A}_1^l \left[\mathbf{A}_1^l + \mathbf{A}_2^l\right]^{-1} \mathbf{A}_1^l \leq \mathbf{C}^* \leq \mathbf{C}^u + \mathbf{A}_1^u \left[\mathbf{A}_1^u + \mathbf{A}_2^u\right]^{-1} \mathbf{A}_1^u, \tag{4.5}$$

where

$$(\mathbf{A}_1^r)_{ijpq} = \langle C(\mathbf{x}) - C^r \rangle_{ijpq} = \left\langle C'^r \right\rangle, \tag{4.6}$$

$$(A_2^r)_{ijpq} = \left\langle C'^r_{ijkl}(\mathbf{x}) \int \Gamma^r_{klmn}(\mathbf{x} - d\mathbf{x}') C'^r_{mnpq}(d\mathbf{x}') d\mathbf{x}' \right\rangle \tag{4.7}$$

$$\Gamma^r_{ijkl} = E^r_{ijkl}\delta(\mathbf{x}) + \frac{1}{4}\left[G^r_{ijkl}(\mathbf{x}) + G^r_{jk,il}(\mathbf{x}) + G^r_{il,jk}(\mathbf{x}) + G^r_{jl,ik}(\mathbf{x})\right], \tag{4.8}$$

$$E^r_{ijkl} = \frac{1}{15\mu^r}\left(9\frac{k^r + 2\mu^r}{3k^r + 4\mu^r} I_{ijkl} - \frac{3k^r + \mu^r}{3k^r + 4\mu^r}\delta_{ik}\delta_{kl}\right), \quad I_{ijkl} = \frac{1}{2}(\delta_{ik}\delta_{jl} + \delta_{il}\delta_{jk}). \tag{4.9}$$

The parameters k^r and μ^r refer, respectively, to the reference bulk and shear moduli of the composite while δ_{ij} is the unit tensor. The terms with superscripts u and l are calculated by using different reference mediums for the two bounds. The superscript $\mathbf{r}$ refers to the reference medium, which is set to u or l for evaluating upper and lower bounds respectively. $\mathbf{x}$ and $\mathbf{x}'$ are spatial points in microstructure, $C(\mathbf{x})$ is the elastic stiffness tensor of the local state associated with spatial position $\mathbf{x}$, and Γ^r is the fourth-rank symmetrized derivative of the Green function, $\mathbf{G}^r$. $\mathbf{A}_1$ and $\mathbf{A}_2$ depend upon 1-point and 2-point statistics respectively.

4.2.2 Perturbation Theory

Perturbation theory provides tools for obtaining both estimates and bounds, however, estimates can be easily incorporated in the MSD framework, as will be explained in the next chapter. Thus the estimate of effective elastic stiffness $\mathbf{C}^*$ from the perturbation theory can be written down as a series sum as [5].

$$\mathbf{C}^* = \mathbf{C}^r + \left\langle \mathbf{C}' \right\rangle - \left\langle \mathbf{C}'\Gamma\mathbf{C}' \right\rangle + (\mathbf{C}'\Gamma\mathbf{C}'\Gamma\mathbf{C}') - \ldots \tag{4.10}$$

Here the reference tensor is chosen as $\mathbf{C}^r = \langle \mathbf{C} \rangle$ and the series can be truncated at term containing the two-point statistics as

$$\mathbf{C}^* = \langle \mathbf{C} \rangle - \left\langle \mathbf{C}'^r(\mathbf{x}) E^r \mathbf{C}'^r(\mathbf{x}) \right\rangle - \left\langle \mathbf{C}'^r(\mathbf{x}) \int_\Omega \mathbf{K}^r(\mathbf{x} - \mathbf{x}') \mathbf{C}'^r(\mathbf{x}' d\mathbf{x}') \right\rangle, \tag{4.11}$$

$$K^r_{ijkl} \approx \frac{1}{2} \left[G^r_{ij,kl} + G^r_{kj,il} \right] \tag{4.12}$$

In this approach one of the limitations is that the evaluation of terms with superscript r depends upon the choice of reference medium. Further, the evaluation of the terms involve solving convoluted integrals.

Modified Perturbation Estimate

Popularly, estimates of the effective elastic properties were calculated using a volume averaged stiffness tensor in the microstructure as the reference value, s.t. $\mathbf{C}^r = \langle \mathbf{C} \rangle$. An alternative value of reference value of the stiffness tensor was proposed by Binci [2], which was a value between the highest and lowest values of the local stiffness tensors among all elements of the local state space $\mathbf{C}' = \frac{1}{2}(\mathbf{C}^u + \mathbf{C}^l)$. The advantages of using this new reference value are

1. The new reference value of the local stiffness tensor extends the application of the perturbation model to large contrast material systems. Here larger contrast means the ratio of Young's modulus is greater then 1.5.

2. With the new reference value, the $\mathbf{E}^r$ and $\mathbf{K}^r$ terms in Eq.(4.11) become independent of microstructure statistics.

3. With $\mathbf{C}' = \frac{1}{2}(\mathbf{C}^u + \mathbf{C}^l)$ property closures cover complete one and two point statistic.

References

[1] Brent L Adams and T Olson. The mesostructureproperties linkage in polycrystals. *Progress in Materials Science*, 43(1):1–87, 1998.

[2] Massimiliano Binci. *A novel spectral framework for second-order homogenization theories*. PhD thesis, Drexel University, 2008.

[3] David T. Fullwood, Stephen R. Niezgoda, Brent L. Adams, and Surya R. Kalidindi. Microstructure sensitive design for performance optimization. *Progress in Materials Science*, 55(6):522–524, 2010.

[4] Zvi Hashin. Analysis of composite materialsa survey. *Journal of Applied Mechanics*, 50(3):481–505, 1983.

[5] E Kröner. Bounds for effective elastic moduli of disordered materials. *Journal of the Mechanics and Physics of Solids*, 25(2):137–155, 1977.

[6] Ekkehart Kröner. *Statistical continuum mechanics*. Springer, 1972.

[7] John R Willis. Variational and related methods for the overall properties of composites. *Advances in applied mechanics*, 21:1–78, 1981.

Chapter 5

Microstructure Sensitive Design

5.1 Introduction

Microstructure sensitive design (MSD)[3], is a mathematical framework, developed to assist in the multi-scale, bottom-up material design ideas that are conceptualized by Materials-by-Design. At the core, MSD is a framework that transforms the second-order homogenization relationships into an efficient spectral (Fourier) space. The literature for this chapter is referred from [2]. A broad overview of steps in MSD are as follows.

1. The material designer first chooses *principal properties* of interest, along with *candidate materials*.

2. A suitable *microstructure* with desired internal structure (including description of phases, grains, fibers etc.) and the topological arrangement (n-point spatial correlations etc.) of these internal structures is defined.

3. The complete space of possible microstructures possible with the internal structure and topology defined in the previous step is created. This set of all possible microstructures is called *microstructure hull*. Usually the dimension of this set will be governed by the number of parameters used to define the microstructure.

4. Next predictions of the macroscale effective properties are obtained by "plugging in" the local state variables of the constituent material phases, and their local properties using

homogenization relations defined in the literature.

5. After all the possible microstructures and related homogenization relations, the relations are exercised over the complete *microstructure hull*, which leads to discovery of set of all possible combinations of of the principal properties. This set is called *property closures*.

6. At this point, if a property combination is chosen, then using the property closure, these properties can be mapped to the optimal material microstructure (usually this is not a one-to-one mapping).

7. Once a suitable theoretical microstructure is discovered from the microstructure hull, an appropriate processing route can be chosen to produce the desired microstructure with desired effective properties. However, this process-structure link is obtained as a set of path-lines, in the microstructure hull and property closure space as shown in Fig.(5.1)

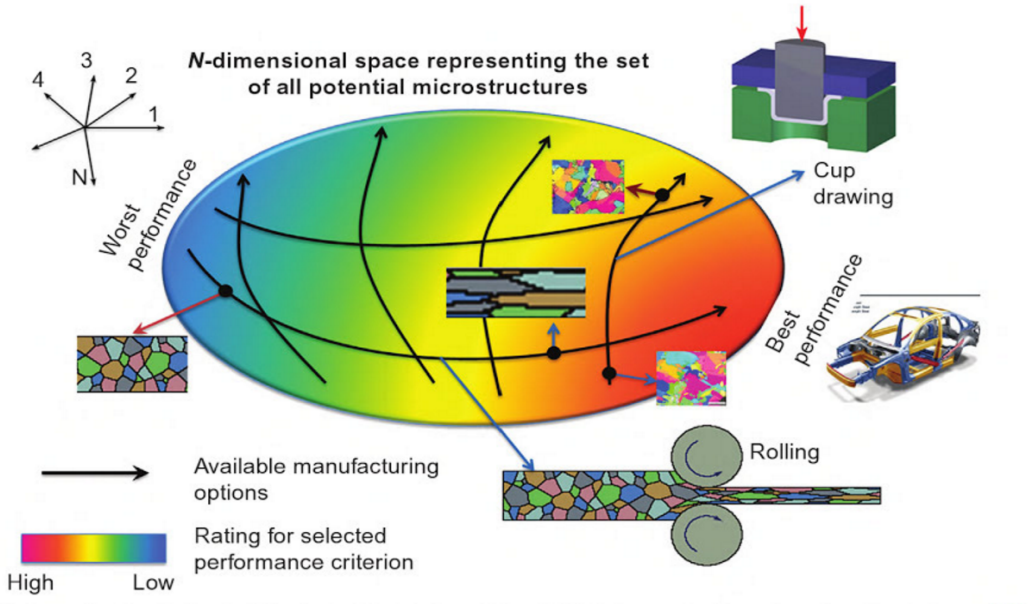

Figure 5.1: Visualization of Property-Structure-Process linkages via path-lines in the microstructure hull and property closure space. Adopted from [5]

A unique offering of MSD framework is that is accounts for material anisotropy at the local state and how it affects the macroscale properties. Spectral representation of second-order linkages defines in the Fourier space a microstructure hull, which contains all feasible microstructures of the selected material system additionally the Fourier decomposition also

reduces the series of convolution integrals of the effective properties into simple algebraic expressions which are computationally more efficient. Further, the decomposed expression includes microstructure parameters that are decoupled from the material parameters, which in turn provide invertibility to the second-order microstructure property linkages.

5.2 Spectral decomposition of Second-Order Homogenization Theories

In this section, we derive the Fourier transform of the second second-order homogenization theories that were discussed in the previous chapter. This decomposition, in the Fourier space sets ground for the microstructure hull, which is the convex region in the Fourier space containing all feasible microstructures and of the material system under consideration. More details about the microstructure hulls is presented in Sec.(5.3).

To begin with decomposition procedure, first we recall the Fourier decomposition of microstructure function shown in Eq.(3.17). Then we can write the 1-point statistics

$$f(\mathbf{h}) = \frac{1}{S}\left(\sum_{s=1}^{S} D_s^n\right)\mathcal{X}^n(\mathbf{h}) \tag{5.1}$$

and the 2-point spatial correlations can be written as

$$f_2(\mathbf{h},\mathbf{h}^{'}|\mathbf{r}) \approx F_t^{nn^{'}}\mathcal{X}^n(\mathbf{h})\mathcal{X}^{n^{'}}(\mathbf{h}^{'})\mathcal{X}_t(\mathbf{r}), \quad F_t^{nn^{'}} = H_{ss^{'}t}D_s^n D_{s^{'}}^{n^{'}}, \tag{5.2}$$

where t enumerates the sub-cells in the partitioning of the $\mathbf{r}$ space, and $H_{ss^{'}t}$ are a set of geometric parameters dependent only on partitioning of the Ω and the $\mathbf{r}$ space. $\Omega|\mathbf{r}$ is the subset of Ω where the points $\mathbf{x}$ and $\mathbf{x}+\mathbf{r}$ lie within Ω.

Now, the first- and second-order probability density functions are introduced in the modified perturbation estimate model presented in Ch.(4).

Recasted effective equation Eq.(4.11)

$$\mathbf{C}^{*} \approx \int_{H} \mathbf{C}(\mathbf{h}) f(\mathbf{h}) d\mathbf{h} - \mathbf{E}^{r} \int_{H} \mathbf{C}^{'r}(\mathbf{h}) \mathbf{C}^{'r}(\mathbf{h}) f(\mathbf{h}) d\mathbf{h},$$
$$- \int_{H} \int_{H} \int_{R(\mathbf{r}_c)} \mathbf{C}^{'r}(\mathbf{h}) \mathbf{K}^{r}(\mathbf{r}) \mathbf{C}^{'r}(\mathbf{h}^{'}) f_2(\mathbf{h}, \mathbf{h}^{'} | \mathbf{r}) d\mathbf{h} d\mathbf{h}^{'} d\mathbf{r}$$

where $R(\mathbf{r}_c)$ denotes the set containing all the distinct vectors that lie in a sphere of radius $\mathbf{r}_c$, known as the coherence length. A strategy to deal with the evaluation of the third term is explained in [6], which is an integration over a sphere of with a radius equal to coherence length, while the microstructure description D_s^n is defined for voxels. Basically, the third term is decomposed into two parts, first one over spatially correlated part and another one over uncorrelated part. After a few algebraic steps following expression for the second-order perturbation estimate of the effective properties of the composite can be written as

$$\mathbf{C}^{*} \approx \mathbf{J}_n^s D_n^s - \aleph_{\mathbf{ss}^{'}}^{\mathbf{nn}^{'}} D_s^n D_{s^{'}}^{n^{'}} \tag{5.3}$$

with

$$\mathbf{J}_s^n = \frac{\mathbf{C}^n}{SN} - \mathbf{E}\frac{\mathbf{C}^{'n}\mathbf{C}^{'n}}{SN}, \tag{5.4}$$

$$\aleph_{ss^{'}}^{nn^{'}} = \frac{Vol(\Omega)}{SN^2} \Xi_t^{nn^{'}} \hat{H}_{ss^{'}t} - \frac{Vol(\Omega)}{S^3N^2} \sum_{p=1}^{S} \sum_{p^{'}=1}^{S} \Xi_t^{nn^{'}} \hat{H}_{pp^{'}t} \tag{5.5}$$

where

$$\Xi_t^{mn^{'}} = \frac{SN^2}{Vol(\Omega)} \int_{H} \int_{H} \int_{R(\Omega)} f(\mathbf{h}, \mathbf{h}^{'} | \mathbf{r}) \mathcal{X}^n(\mathbf{h}) \mathcal{X}^{n^{'}}(\mathbf{h}^{'}) \mathcal{X}_t(\mathbf{r}) d\mathbf{h} d\mathbf{h}^{'} d\mathbf{r} \tag{5.6}$$

$$\tag{5.7}$$

and,

$$f(\mathbf{h}, \mathbf{h}^{'} | \mathbf{r}) = \mathbf{C}^{'r}(\mathbf{h}) \mathbf{K}^{r}(\mathbf{r}) \mathbf{C}^{'r}(\mathbf{h}^{'}) \approx \aleph_t^{nn^{'}} \mathcal{X}^n(\mathbf{h}) \mathcal{X}^{n^{'}}(\mathbf{h}^{'}) \mathcal{X}_t(\mathbf{r}) \tag{5.8}$$

The microstructure variables in Eq.(4.15) are subject to constraint mentioned in Eq.(3.19). So applying the constraint in Eqs.(5.3)-(5.5) allows further compaction of the microstructure space from SN dimensions to $S(N-1)$ dimensions. Thus, the modified microstructure-effective property relationship can be written as

$$\hat{\mathbf{C}}^* = \sum_{s=1}^{S}\sum_{n=1}^{N-1}\hat{\mathbf{B}}_s^n D_s^n - \sum_{s=1}^{S}\sum_{s'=1}^{S}\sum_{n=1}^{N-1}\sum_{n'=1}^{N-1}\hat{\mathbf{A}}_{ss'}^{nn'} D_n^s D_{s'}^{n'}, \tag{5.9}$$

with

$$D_s^n \geq 0 \quad \forall n = 1 \dots N \tag{5.10}$$

and

$$\hat{\mathbf{A}}_{ss'}^{nn'} = \aleph_{ss'}^{nn'} - \aleph_{ss'}^{nN} - \aleph_{ss'}^{Nn'} + \aleph_{ss'}^{NN}, \tag{5.11}$$

$$\hat{\mathbf{B}}_s^n = \mathbf{J}_s^n - \mathbf{J}_s^N - N\sum_{s'=1}^{S}\left(\aleph_{ss'}^{nN} - 2\aleph_{ss'}^{NN} + \aleph_{ss'}^{Nn}\right), \tag{5.12}$$

$$\hat{\mathbf{C}}^* = \hat{\mathbf{C}}^* - N\sum_{s=1}^{S}\mathbf{J}_s^N + N^2\sum_{s=1}^{S}\sum_{s'=1}^{S}\aleph_{ss'}^{NN} \tag{5.13}$$

This is the final spectral formulation of the effective properties.

5.3 Spectral representation of Orientation Distribution Function (ODF)

In this section only the main expressions for spectral representation are presented as these will be used later for decomposition of homogenization theories.

The ODF can be expanded as a Fourier series using generalized spherical harmonic (GSH) basis functions, T_l^{mn}, as

$$f(g) = \sum_{l=0}^{\infty}\sum_{m=-l}^{+l}\sum_{n=-l}^{+l} F_l^{mn} T_l^{mn}(g) \tag{5.14}$$

For representing ODF using DFT, we transform the orientation space to a distortion-free space defined by $(\phi_1, \mathbf{\Phi}, \phi_2)$ [3]. Then for a periodic domain of interest the 3D Bunge-Euler

space in divided into a $B_1xB_2xB_3$ grid, and let (b_1, b_2, b_3) enumerate the grid points. So the DFT representation of ODF is defined as

$$f_{b_1b_2b_3} = \frac{1}{B_1B_2B_3} \sum_{k_1=0}^{B_1-1} \sum_{k_2=0}^{B_2-1} \sum_{k_3=0}^{B_3-1} F_{k_1k_2k_3} e^{\frac{2\pi i k_1 b_1}{B_1}} e^{\frac{2\pi i k_2 b_2}{B_2}} e^{\frac{2\pi i k_3 b_3}{B_3}} \tag{5.15}$$

where $f_{b_1b_2b_3}$ denote the value of the ODF at the grid point (b_1, b_2, b_3).

5.4 Microstructure Hull and its Reduced Order Representation

The concept of the convex and compact microstructure hull was introduced by Adams et. al (Adams et al., 2001). The advantage of a convex and compact representation is that, each point in the hull represents a unique microstructure and all points outside the hull are non-physical. The lines on the hull as seen in Fig.(3.7) represent linear combinations of microstructures at the endpoints.

Mathematically, a continuous ODF can be defined in terms of the discrete set of crystals using delta functions (Fullwood et. al, 2010).

$$f(g) = \sum_k a_k \delta(g - g^k), \quad 0 \leq a_k \leq 1, \quad \sum_k a_k = 1 \tag{5.16}$$

where the Dirac-delta function, $\delta(g - g^k)$, represents the oDF of a single crystal of orientation g^k, with $a_k$denoting volume fraction in a polycrystal.

As seen in Sec.(3.2), the ODF can be expressed as a Fourier series using GSH basis function $T_l^{\mu\nu}$. This gives us the opportunity to visualize the ODF as a point in an infinite dimensional space, whose axes are defined by Fourier coefficient $F_l^{\mu\nu}$ and the coordinates of the point are given by the corresponding value of $F_l^{\mu\nu}$ as seen in Fig.(3.7).

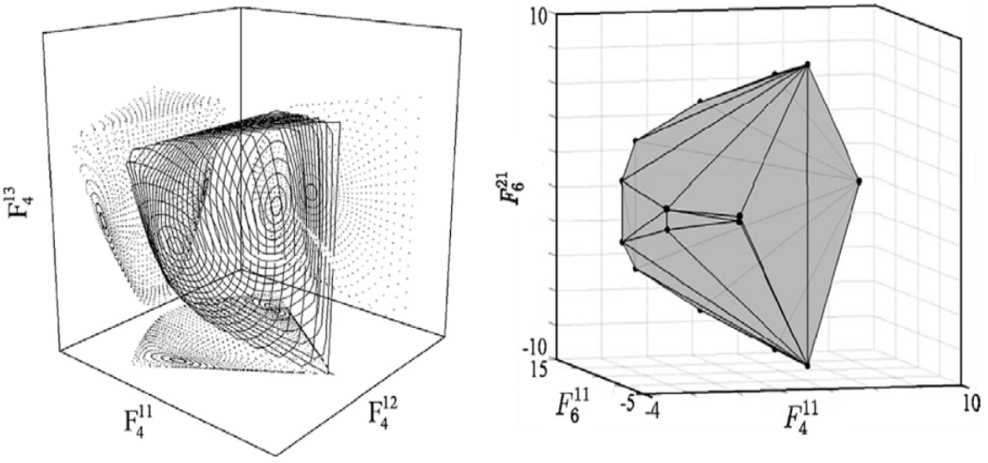

Figure 5.2: Left: representation of the texture hull for cubic-orthorhombic materials in the rst three dimensions of the Fourier space. Right: the hexagonalorthorhombic texture hull projected in the three dominant dimensions of the Fourier space. Image courtesy [3]

Now a convex compact microstructure hull [], in terms of Fourier coefficients can be written as

$$M = \left\{ F_l^{\mu\nu} | F_l^{\mu\nu} = \sum_k a_k^k F_l^{\mu\nu}, {}^k F_l^{\mu\nu} \in M^k, a_k \geq 0, \sum_k a_k = 1 \right\} \tag{5.17}$$

where

$$M^k = \left\{ {}^k F_l^{\mu\nu} | {}^k F_l^{\mu\nu} = \frac{1}{2l+1} \ddot{T}_l^{\mu\nu *}(g^k) \right\} \tag{5.18}$$

where the asterik operator denotes complex conjugate.

In a 1-point hull, a single point represents all microstructures with same ODF. Higher order statistics such as spatial correlations can be captured in the hull, need higher-order hulls. Construction procedure of higher-order hulls of a composite system is outlined in [2, 9, 7].

5.5 Property Closures

As briefly mentioned in the opening section of this chapter, *property closures* enable solving the inverse problem i.e. they help the material designer identify the feasible range of the combination of selected properties of interest in a given material system.

Delineation of first order property closures of two effective anisotropic elastic-plastic properties **P** and **Q** can be visualized through following steps

1. Identify the subset of microstructure hulls that are theoretically predicted to correspond to a selected value of one of the effective property (say, P=$\tilde{P}$).

2. From this subset of microstructures, the maximum and minimum values of Q that are theoretically feasible.

3. Explore $\tilde{P}$ between its own theoretically feasible maximum and minimum values, to complete the first-order property closure

First order closures for a broad range of cubic materials, can be seen in Fig.(5.2). These correspond to the effective modulus in uniaxial strain and the effective shear modulus in a sample.

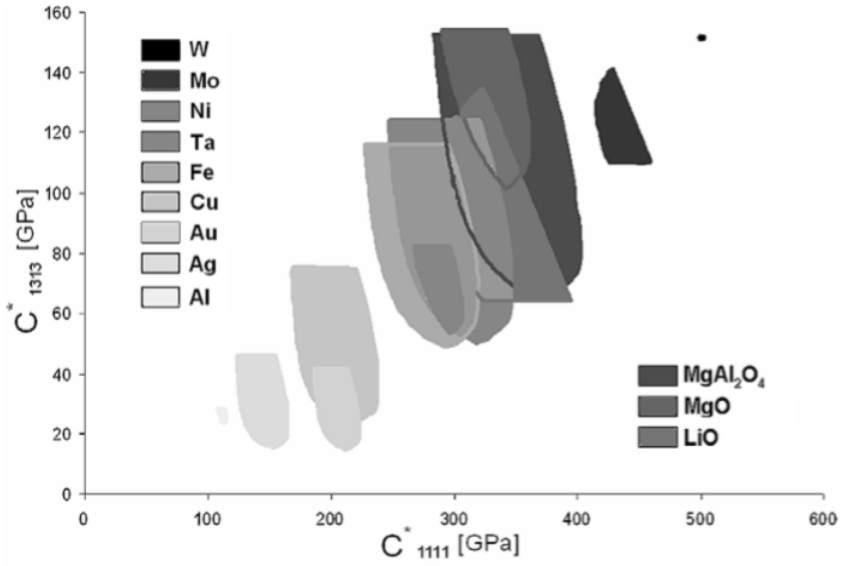

Figure 5.3: Atlas of (C^*_{1111}, C^*_{1313}) first-order closures for a broad selection of cubic materials.Image courtesy [3]

The procedure of delineating Second-Order property closures was introduced by Binci (Binci and Kalidindi, 2008). In this procedure components (say $\mathbf{P}$ and $\mathbf{Q}$) of effective stiffness tensor are evaluated using Eq.(5.9). Then the complete range of feasible effective property combinations $(\mathbf{P}^*, \mathbf{Q}^*)$ defines the second-order property closures.

5.6 Spectral formulation for Localization Tensors

The main aim of the localization relationships is to connect the macroscale loading to the microscale response. Structure-property linkages are established through a fourth-rank localization tensor which is derived from second-order homogenization theory. For instance, a loading at macro-scale can be connected to local elastic properties such as stress and strain.

Building upon the spectral representation of microstructure function presented in Sec.(3.3.1), now we introduce the spectral representation of *localization tensors*. Localization tensors establish the linkages between different hierarchical scales occurring in materials. These linkages provide efficient scale-bridging relationships of microstructure parameters defined at different length scales. The localization tensors are proven to be computationally more efficient then FEM models in predicting local properties of composites [1, 8, 4]. This is accomplished by recasting the localization tensors into a Fourier space, which decouples the microstructure coefficients from other parameters known as influence coefficients (see chapter 5). The main expressions for calculating *influence coefficients* are written next (for details of the derivation see (Binci and Kalidindi, 2008)).

The fourth-rank localization tensor, $\mathbf{a}$, links the response local elastic strain to any strain imposed on the macroscale as

$$\epsilon(\mathbf{x}) = \mathbf{a}(\mathbf{x}) \left\langle \epsilon(\mathbf{x}) \right\rangle , \tag{5.19}$$

$$\mathbf{a}(\mathbf{x}) = \mathbf{I} - \left\langle \mathbf{\Gamma}^{'}(\mathbf{x}, \mathbf{x}^{'}) \mathbf{C}^{'}(\mathbf{x}^{'}) \right\rangle + \left\langle \mathbf{\Gamma}^{r}(\mathbf{x}, \mathbf{x}^{'}) \mathbf{C}^{'}(\mathbf{x}^{'}) \mathbf{\Gamma}^{r}(\mathbf{x}^{'}, \mathbf{x}^{''}) \mathbf{C}^{'}(\mathbf{x}^{''}) \right\rangle - \dots \tag{5.20}$$

where $\mathbf{I}$ is the fourth-rank identity tensor, $\mathbf{C}^{'}(\mathbf{x})$ is the deviation in the local stiffness at spatial location $\mathbf{x}$ w.r.t that of a selected reference medium, $\mathbf{\Gamma}^{r}$ is a symmetrized derivative of the Green's function defined using the elastic properties of the selected reference media, and $\langle\rangle$ brackets represent ensemble averages over RVE. The first $\langle\rangle$ on the right hand side captures the contribution to the tensor $\mathbf{a}(\mathbf{x})$ from a particular local state at point $\mathbf{x}^{'}$. Thus by evaluating the localization tensor at different $\mathbf{x}^{'}$ in the material and taking an average, the contribution from the *local* 2-point statistics of the microstructure is captured. Similarly, the second $\langle\rangle$ term in Eq.(5.16) reflects contribution of two local states at points $\mathbf{x}^{'}$ and $\mathbf{x}^{''}$.

However, there are underlying problems in direct evaluation of terms in Eq.(5.15). The first problem is the evaluation of the convolution integrals with singular integrands and the secondly, the solution obtained once would need to reevaluated for every change in microstructure. The spectral method resolves these problems and provides an efficient

Recalling, the Fourier representation of the microstructure function, considering orientation and spatial dependence separately, as

$$M(\mathbf{x}, \mathbf{h}) \approx D_s^n \mathcal{X}_s(\mathbf{x}) \mathcal{X}^n(\mathbf{h}) \tag{5.21}$$

where D_s^n are the microstructure coefficients, $\mathcal{X}_s(\mathbf{x})$ and $\mathcal{X}^n(\mathbf{h})$ are the primitive basis as noted in Sec.(3.1.1)

The real space and the local state space H with primitive basis is equivalent to tessellation of the RVE into cuboids $\omega_s (s = 1 \dots S)$, as shown in Fig.(5.2.a),and to the tessellation of the space H into bins $\gamma_n (n = 1 \dots N)$.

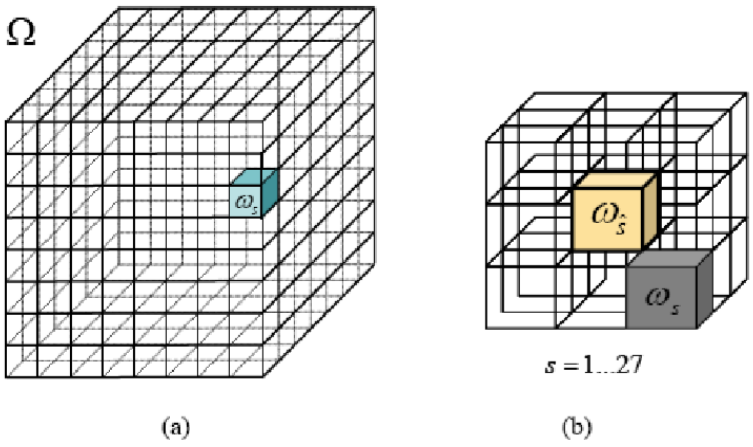

Figure 5.4: (a) Tesselation of the RVE into cuboids $\omega_s (s = 1 \dots S)$ (b)Cluster of first neighboring volume bins used in the truncated spectral representation of the localization tensor. Image courtesy [2]

Now to transform the Eq.(5.15) into Fourier space, first we write the local elastic stiffness in terms of microstructure function as

$$\mathbf{C}'(\mathbf{x}) = \int_H \mathbf{C}'(\mathbf{h}) M(\mathbf{x}, \mathbf{h}) d\mathbf{h} \tag{5.22}$$

where $\mathbf{C}^{'}(\mathbf{h})$ is the deviation in elastic stiffness of the local state $\mathbf{h}$ as compared to the reference medium, and can be represented in Fourier space $\mathbf{C}^{'}(\mathbf{h}) \approx \mathbf{C}^{'n}\mathcal{X}^{n}(\mathbf{h})$ and $\mathbf{C}^{'n}$ is the average deviation of elastic stiffness tensor of local states γ_n from reference medium.

Replacing Fourier decomposition of microstructure function and deviation in elastic stiffness into Eq.(5.17), we get

$$\mathbf{C}^{'}(\mathbf{x}) \approx \int_{H} \mathbf{C}^{'n^{'}} \mathcal{X}^{n^{'}}(\mathbf{h}) D_S^n \mathcal{X}(\mathbf{x}) \mathcal{X}^{n}(\mathbf{h}) d\mathbf{h} = \frac{1}{N} \mathbf{C}^{'n} D_S^n \mathcal{X}_s(\mathbf{x}) \tag{5.23}$$

The term $\Gamma^{r}(\mathbf{x}, \mathbf{x}^{'})$ in Eq.(5.15), can be decomposed as

$$\mathbf{\Gamma^{r}}(\mathbf{x}, \mathbf{x}^{'}) = \mathbf{K}^{r}\delta(\mathbf{x} - \mathbf{x}^{'}) + \xi^{r}\mathbf{\Phi}(\mathbf{x} - \mathbf{x}^{'}) + \eta^{r}\mathbf{\Psi}(\mathbf{x} - \mathbf{x}^{'}) \tag{5.24}$$

where δ represents the Dirac delta function. Further, spatial dependence of functions can be expressed in Fourier space as

$$\delta(\mathbf{x} - \mathbf{x}^{'}) \approx \delta_{SS'} \mathcal{X}_S(\mathbf{x}) \mathcal{X}_S^{'}(\mathbf{x}^{'}), \tag{5.25}$$

$$\mathbf{\Phi}(\mathbf{x} - \mathbf{x}^{'}) \approx \mathbf{\Phi}_{SS'} \mathcal{X}(\mathbf{x}) \mathcal{X}_{S'}(\mathbf{x}^{'}), \tag{5.26}$$

$$\mathbf{\Psi}(\mathbf{x} - \mathbf{x}^{'}) \approx \mathbf{\Psi} \mathcal{X}_S(\mathbf{x}) \mathcal{X}_{S'}(\mathbf{x}^{'}) \tag{5.27}$$

with,

$$\mathbf{\Phi}_{SS'} = \left(\frac{S}{Vol(\Omega)}\right)^2 \int_{\Omega}\int_{\Omega} \mathbf{\Phi}(\mathbf{x} - \mathbf{x}^{'}) \mathcal{X}_S(\mathbf{x}) \mathcal{X}_{S'}(\mathbf{x}^{'}) d\mathbf{x}^{'} d\mathbf{x}, \tag{5.28}$$

$$\mathbf{\Psi}_{SS'} = \left(\frac{S}{Vol(\Omega)}\right)^2 \int_{\Omega}\int_{\Omega} \mathbf{\Psi}(\mathbf{x} - \mathbf{x}^{'}) \mathcal{X}_S(\mathbf{x}) \mathcal{X}_{S'}(\mathbf{x}^{'}) d\mathbf{x}^{'} d\mathbf{x} \tag{5.29}$$

Finally, we can write the spectral decomposition as

$$\mathbf{\Gamma}^{r}(\mathbf{x}, \mathbf{x}^{'}) \approx \mathbf{\Gamma^{r}_{SS'}} \mathcal{X}_S(\mathbf{x}) \mathcal{X}_{S'}(\mathbf{x}^{'}) \tag{5.30}$$

Now, the localization tensor can be written as

$$\mathbf{a}(\mathbf{x}) = \mathbf{x}_{\hat{S}} \mathcal{X}_{\hat{S}}(\mathbf{x}) \tag{5.31}$$

Now the first terms of Eq.(5.15), that represents contribution of 2-point correlations can be written as,

$$\left\langle \mathbf{\Gamma}(\mathbf{x}, \mathbf{x}^{'}) \mathbf{C}^{'}(\mathbf{x}^{'}) \right\rangle = \int_{\Omega} \mathbf{\Gamma}^{r}(\mathbf{x}, \mathbf{x}^{'}) \mathbf{C}^{'}(\mathbf{x}^{'}) d\mathbf{x}^{'} \approx \frac{Vol(\Omega)}{NS} \mathbf{\Gamma}^{r}_{\hat{S}S} \mathbf{C}^{'n} D^{n}_{S} \mathcal{X}_{\hat{S}}(\mathbf{x}) \tag{5.32}$$

second term in the expansion represents contribution of 3-point correlations and can be written as

$$\left\langle \mathbf{\Gamma}^{r}(\mathbf{x}, \mathbf{x}^{'}) \mathbf{C}^{'}(\mathbf{x}^{'}) \mathbf{\Gamma}^{r}(\mathbf{x}^{'}, \mathbf{x}^{''}) \mathbf{C}^{'}(\mathbf{x}^{''}) \right\rangle = \int_{\Omega} \mathbf{\Gamma}^{r}(\mathbf{x}, \mathbf{x}^{'}) \mathbf{C}^{'}(\mathbf{x}^{'}) \int_{\Omega} \mathbf{\Gamma}^{r}(\mathbf{x}^{'}, \mathbf{x}^{''}) \mathbf{C}^{'}(\mathbf{x}^{''}) d\mathbf{x}^{''} d\mathbf{x}^{'} \approx$$
$$\approx \left(\frac{Vol(\Omega)}{NS} \right)^{2} \mathbf{\Gamma}^{r}_{\hat{S}a} \mathbf{C}^{'n} \mathbf{\Gamma}^{r}_{bS^{'}} \mathbf{C}^{'n^{'}} \delta_{Sab} D^{n}_{S} D^{n^{'}}_{S^{'}} \mathcal{X}_{\hat{S}(\mathbf{x})} \tag{5.33}$$

where δ is Kronecker delta. Finally, substituting Eqs.(5.26)-(5.28) in Eq.(5.15) we get the quadratic expression

$$\mathbf{a}_{\hat{s}} = \mathbf{I} - \mathbf{J}^{n}_{\hat{S}S} D^{n}_{S} + \mathbf{L}^{nn^{'}}_{\hat{S}SS^{'}} D^{n}_{S} D^{n^{'}}_{S^{'}} \tag{5.34}$$

where,

$$\mathbf{J}^{n}_{\hat{S}S} = \frac{Vol(\Omega)}{NS} \left[\mathbf{K}^{r} \mathbf{C}^{'n} \delta_{\hat{S}S} + \left(\chi^{r} \Phi_{\hat{S}S} + \eta^{r} \Psi_{\hat{S}S} \right) \mathbf{C}^{'n} \right], \tag{5.35}$$

and

$$\mathbf{L}^{nn^{'}}_{\hat{S}SS^{'}} = \left(\frac{Vol(\Omega)}{NS} \right)^{2} . \Big(\mathbf{K}^{r} \mathbf{C}^{'n} \mathbf{K}^{r} \mathbf{C}^{'n^{'}} \delta_{\hat{S}SS^{'}} +$$
$$\mathbf{K}^{r} \mathbf{C}^{'n} \left(\chi^{r} \Phi_{bS^{'}} + \eta^{r} \Psi_{bS^{'}} \right) \mathbf{C}^{'n^{'}} \delta_{\hat{S}Sb} +$$
$$\left(\delta^{r} \Psi_{\hat{S}a} + \eta^{r} \Psi_{\hat{S}a} \right) \mathbf{C}^{'n} \mathbf{K}^{r} \mathbf{C}^{'n^{'}} \delta_{\hat{S}aS^{'}} +$$
$$\left(\delta^{r} \Psi_{\hat{S}a} + \eta^{r} \Psi_{\hat{S}a} \right) \mathbf{C}^{'n} \left(\delta^{r} \Psi_{bS^{'}} + \eta^{r} \Psi_{bS^{'}} \right) \mathbf{C}^{'n^{'}} \delta_{Sab} \Big) \tag{5.36}$$

where $\mathbf{J}^{n}_{\hat{S}S}$ and $\mathbf{L}^{nn^{'}}_{\hat{S}SS^{'}}$ are referred to as the *influence coefficients*. These coefficients quantify the

influence of presence of local states n and $n^{'}$ in bins S and $S^{'}$, on bin $S^{'}$.

The sensitivity of the localization tensor in bin $\hat{S}$ to changes in specific microstructure coefficients can be given by

$$\frac{\partial a_{\hat{S}}}{\partial D_S^n} = -\mathbf{J}_{\hat{S}S}^n + \left(\mathbf{L}_{\hat{S}SS'}^{nn'} + \mathbf{L}_{\hat{S}S'S}^{n'n}\right) D_{S'}^{n'} \tag{5.37}$$

References

[1] Hamad F Al-Harbi, Giacomo Landi, and Surya R Kalidindi. Multi-scale modeling of the elastic response of a structural component made from a composite material using the materials knowledge system. *Modelling and Simulation in Materials Science and Engineering*, 20(5):055001, 2012.

[2] Massimiliano Binci. *A novel spectral framework for second-order homogenization theories*. PhD thesis, Drexel University, 2008.

[3] David T. Fullwood, Stephen R. Niezgoda, Brent L. Adams, and Surya R. Kalidindi. Microstructure sensitive design for performance optimization. *Progress in Materials Science*, 55(6):522–524, 2010.

[4] Akash Gupta, Ahmet Cecen, Sharad Goyal, Amarendra K Singh, and Surya R Kalidindi. Structure–property linkages using a data science approach: Application to a non-metallic inclusion/steel composite system. *Acta Materialia*, 91:239–254, 2015.

[5] Surya R Kalidindi. *Hierarchical Materials Informatics: Novel Analytics for Materials Data*. Elsevier, 2015.

[6] Surya R Kalidindi, Hari K Duvvuru, and Marko Knezevic. Spectral calibration of crystal plasticity models. *Acta Materialia*, 54(7):1795–1804, 2006.

[7] Surya R. Kalidindi, Giacomo Landi, and David T. Fullwood. Spectral representation of higher-order localization relationships for elastic behavior of polycrystalline cubic materials. *Acta Materialia*, 56(15):3843–3853, 2008.

[8] Surya R. Kalidindi, Stephen R. Niezgoda, Giacomo Landi, Shraddha Vachhani, and Tony Fast. A novel framework for building materials knowledge systems. *CMC*, 17(2):103–125, 2010.

[9] Stephen Richard Niezgoda. *Stochastic representation of microstructure via higher-order statistics: theory and application*. 2010.

Chapter 6

Material Knowledge Systems

6.1 Introduction

Building upon the concepts described in previous chapters, now we discuss the Material Knowledge System [3], which is described as *a computational framework to extract, store and recall hierarchical PSP linkages for a broad range of material systems* by [6]. MKS uses Digital Signal Processing (DSP) methods establish relations between microstructure topologies and field response variables of the material (Shan and Wang, 2010). Using the expressions derived in Eqs.(5.17)-(5.19) and analogous of the concept in DSP the localization of the field response variables can be noted as a series of higher-order convolutions connecting structure and response signals as:

$$\frac{P_S}{\bar{P}} = \left(\sum_{h=1}^{H} \sum_{\mathbf{t} \in \mathbf{S}} \alpha_{\mathbf{t}}^{h} m_{S+\mathbf{t}}^{h} + \sum_{h=1}^{H} \sum_{h'=1} \sum_{\mathbf{t} \in S} \sum_{\mathbf{t}' \in S} \alpha_{\mathbf{t}\mathbf{t}'}^{hh'} m_{\mathbf{S}+\mathbf{t}}^{h} m_{\mathbf{S}+\mathbf{t}+\mathbf{t}'}^{h'} + \dots \right) \tag{6.1}$$

Where P_S is the digital representation of local response field of interest (e.g. local stress, strain, etc.). The subscript S represents the spatial cell where the local response field is being calculated. The first and second order influence coefficients represented by α_t^h and $\alpha_{tt'}^{hh'}$ respectively, are fourth-rank tensors and are completely independent of microstructure coefficients m_s^h.

For a selected materials system, α_t^h essentially captures the influence of a local state h placed

at a distance t on the spatial cell S of interest. As expected, $\alpha_{tt'}^{hh'}$, which includes higher order statistics about the microstructure, captures the influence of simultaneous placement of local states h and h' at a distance of $S+t$ and $S+t+t'$ on the spatial cell of interest.

The *influence coefficients* also known as impulse filters described in the last chapter, can infer the local effect of microstructure structure on the local material response. The learning or calibration of these influence coefficients is done once for a selected composite material system, as the coefficients are independent of the morphology of the underlying microstructure.

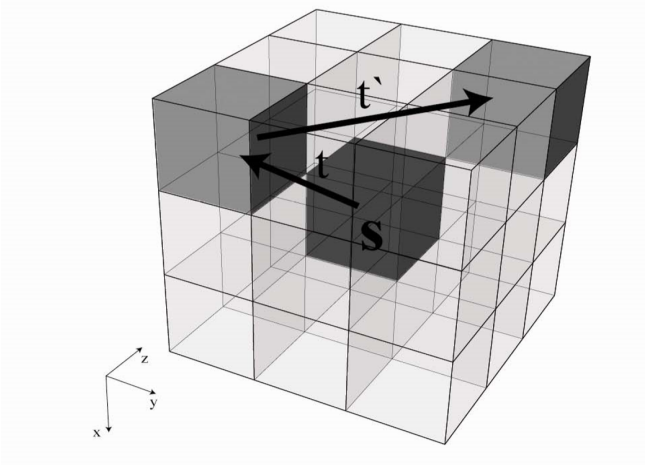

Figure 6.1: The first-order influence coefficients α_t^h capture the contribution of the response variable in spatial cell S from the placement of local state h in spatial bins $S+t$. Similarly, $\alpha_{tt'}^{hh'}$ captures the influence of placement of h and h' in spatial bins $S+t$ and $S+t+t'$.Image courtesy [8]

Classical approach to calculate influence coefficients as per statistical continuum theory is analytical. However, this approach poses computational challenges. To overcome this challenge Landi and coworkers [1] and [2, 5] established a more efficient way of obtaining numerical values for these coefficients, by calibrating it against finite element (FE) models. Another limitation of the existing formulation is that, the influence coefficients are coupled. To simplify, a decoupling process by using convolution properties of DFT was proposed as

$$P_k = \left[\left(\sum_{h=1}^{H} \beta_k^{h*} M_k^h \right) + \left(\sum_{h=1}^{H} \sum_{h'=1}^{H} \sum_{\mathbf{r} \in S} \beta_{\mathbf{kr}}^{hh'*} M_{\mathbf{r}}^{h'} M_{\mathbf{k-r}} \right) + \dots \right] \tag{6.2}$$

$$\beta_k^h = \Im\left(\alpha_{\mathbf{t}}^h\right), \quad P_{\mathbf{k}} = \Im(p_S/\hat{p}), \quad M_{\mathbf{k}}^h = \Im_{\mathbf{k}}(m_s^h) \tag{6.3}$$

where $\Im_{\mathbf{k}}()$ denotes the multi-dimensional DFT operation w.r.t. spatial variables $\mathbf{t}$ or $\mathbf{s}$, and asterisk represents complex conjugate. This new formulation decouples the coefficients and makes their calibration against FE models computationally efficient.

The first-order MKS have been used accurately for plastic-responses, elastic stress and strain fields, and thermo-elastic. With first-order system, only two discrete phases with weak contrast between their Poisson ratio and Young's modulus.

However, there is a need to incorporate higher-order influence coefficients in order to improve accuracy. The Fourier transform isn't efficient because it can't decouple the higher-order localization relationship. If it is done in any case, there will be a need to include every higher-order term up to $N-th$ order, which makes it unfeasible computationally.

6.2 Higher Order MKS

A new methodology to incorporate higher-order coefficients and thus more information of the microstructure topology was proposed by Fast [3].

6.2.1 Higher Order Microstructure Function

First the higher-order microstructure equation is modified to be written as

$${}_l m_{S+t_i}^{\tilde{h}} = m_{S+t_1}^{h_1} m_{S+t_1+t_2}^{h_2} \dots m_{S+t_1+\dots+t_N}^{h^N} \tag{6.4}$$

where $\tilde{h}$ is the local state identifier, thus $(h_1, \dots, h_N)$ are ordered set of combination of local states and $\tilde{H}$ being the product space of individual local state variables. .

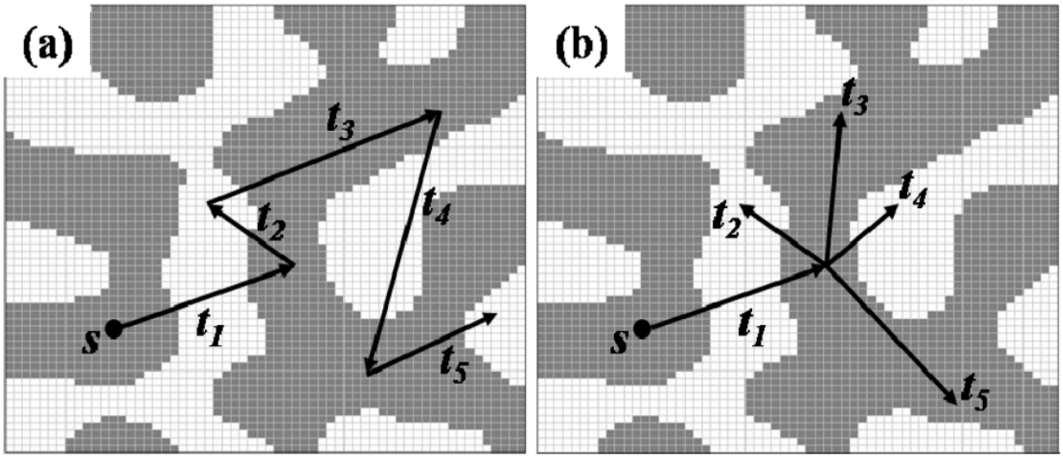

Figure 6.2: (a) Illustration of higher-order terms in localization relationship, where all selected vectors are independent of all others. (b) Illustration of higher order terms in reformulated localization relationship presented in [3]

6.2.2 Generalized Localization Relationship

When the constraint on number of local states is removed, the first-order localization relationship generalizes to

$$p_s = \sum_{h=1}^{H} \sum_{t=0}^{S-1} \alpha_t^h m_{s+t'} \tag{6.5}$$

here H is upper bounded LSS indices takes a value s.t. $H \geq 2$.

6.2.3 Higher Order Localization Relationship

Using higher-order microstructure function definition from Eq.(6.4) in Eq. (6.5) we get

$$p_s = \sum_{i=1}^{l} \sum_{h=1}^{H} \sum_{t_1=0}^{S-1} {}^i\alpha_{t_1}^h \, {}^i m_{S+t_1}^h + e_S(I) \tag{6.6}$$

${}^i\alpha_l^{\mu\nu}$ is the compact notation of influence-coefficients of higher-order with the local vectors indexed by i, and truncation error is given by $e_S(I)$.

6.3 Applications of MKS

Integrated Computational Materials Engineering (ICME) project is focused on multiscale modelling of materials and developing schemes for effective communication between constitutive models at different length scales. This is inline with the fact that, material structure is naturally hierarchical, with varying length and time scales at each step of the hierarchy. Development of multiscale modelling techniques will enable faster design, development and accelerated material discovery for insertion into existing manufacturing processes. Multiscale modelling can be basically divided into two classes, hierarchical and concurrent.

In the Hierarchical modelling approach, scale bridging relationships are used to transfer information from one scale to another. The main advantage of hierarchical simulations over concurrent modelling is the saving in computational effort. However, for achieving higher computational efficiency, hierarchical modelling compromises on accuracy by incorporating simplifying assumptions about the material. On the other hand, concurrent modelling, although more accurate, but are computationally very expensive as constitutive models are solved simultaneously at all the length scales while exchanging information continuously.

For the purpose of this thesis, we will focus on Hierarchical modelling, due to it's relatively easier implementation and lesser requirements for computational power. Until recently, the primary focus of hierarchical modelling has been on Homogenization, thus the information flow has been usually one sided i.e., from lower to higher scales. Therefore, the localization problem is relatively not well addressed. As discussed in previous chapters, Localization techniques can provide the spatial distribution of local response fields of interest (local stresses, strains etc.), resulting from a macroscale boundary condition/loading.

MKS scale-bridging framework has been successfully implemented in several case studies for determining the localized response fields ([6, 7, 3]). In a nutshell, MKS addresses the localization problem by using better statistical measures, i.e. n-point spatial correlations, of the microstructures.

Now using the theory and concepts we have laid out in earlier chapters, we will use the MKS framework for a case study where we evaluate the elastic response of a three-dimensional

voxel-based microstructure dataset using novel DFT-based knowledge systems as described in [9].

6.3.1 Numerical Example: Elastic response of a composite material system.

In this case study, DFT-based localization relationship is used to calculate the elastic response of a 3D voxel based dataset comprising of two different phases. Both the phases have isotropic elastic properties, with Young's moduli of 200 and 300 GPa respectively. The ratio of modulis is 1.5 which means its a medium contrast material. Poisson ratio for both phases is chosen 0.3.

Selection of microstructure for influence coefficient calibration.

In order to estimate the influence coefficients as shown in Eq.(6.2), we create and use a FE model of a delta microstructure (see Fig.(7.1)) in Abaqus[4]. The Abaqus *.inp* file used to create this model can be seen in Appendix.

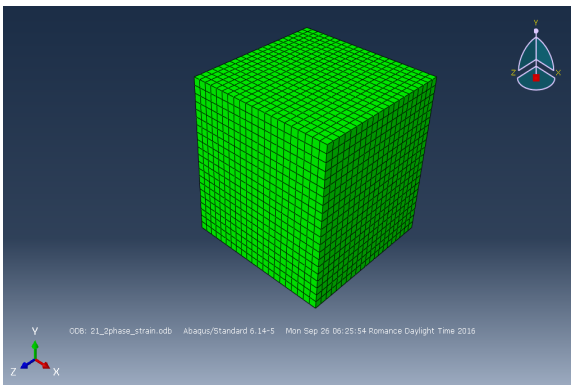

Figure 6.3: Finite element model of Delta microstructure of size 21x21x21, resulting in a total of 9361 C3D8 type elements.

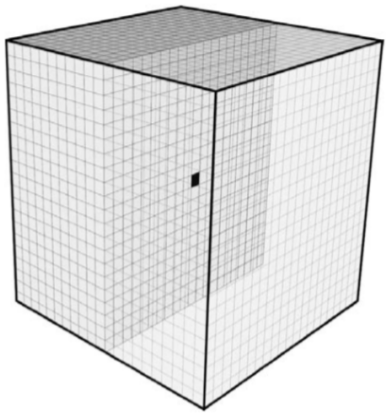

Figure 6.4: Delta microstructure used in this numerical example. Image courtesy [7]

The delta microstructure is the one where one of the local state occupies the central spatial bin, and is completely surrounded by the other local state as shown in Fig.(7.2). Landi [9] established that use of delta microstructures is specially suited for using DFTs. This is primarily because delta microstructures function in m_s^h produces non-zero values of M_k^h. Moreover, in the field of digital signal processing a well defined methodology is to identify output for an impulse

(delta microstructure in our case) and then outputs are obtained as a convolution of the impulse input signal.

The FE model was created in Abaqus[4], with 3-D, eight noded solid elements (C3D8). The cubic elements closely resemble the voxel based discretization of microstructures, thus such meshes can be produced naturally from microstructure datasets. The domain in comprised of 21x21x21 = 9261 elements as can be seen in Fig.(7.1).

Boundary conditions for FE analyses

For this problem we will consider estimation of the $(\beta_k^h)_{ij11}$ component of the fourth rank tensor β_k^h same as the α_t^h tensor. For estimation of this coefficient a uniaxial strain is applied at the macroscale, and the spatial variation of the response strain components are documented in the Abaqus *.dat* file (see Appendix), while all the other strain components are kept equal to zero. Periodic boundary conditions are applied to the FE model, which are as follows

$$u_i^{3+} = u_i^{3-}, \quad u_i^{2+} = u_i^{2-}, \quad u_{i\neq 3}^{1+} = u_{i\neq 3}^{1-}, \quad u_3^{1+} - u_3^{1-}, \quad u_i^B = 0 \tag{6.7}$$

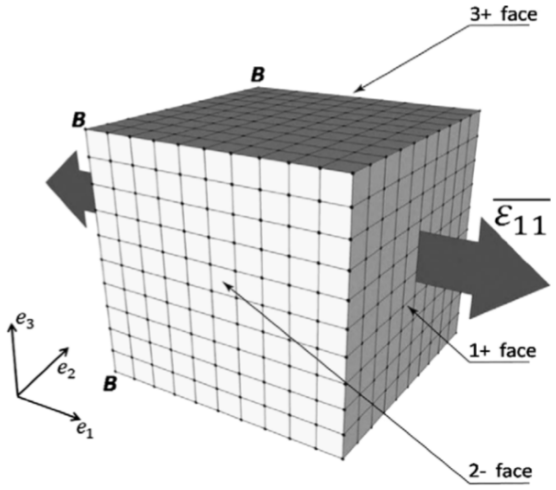

Figure 6.5: Periodic boundary conditions are applied using conditions described in Eq.(7.1).

Imosing periodic bcs, ensures that the equations are set up in a way that, displacements of nodes on opposite faces are related. Details of the surfaces and boundary conditions can be visually verified from Fig. (7.3)

Establishing the first-order coefficients

Recalling the procedure described, in order to establish $(\beta_k^h)_{ij11}$ in the previous chapters. The first order coefficients can be calculated as

$$(e_{ij})_k = \left(\sum_{h=1}^{H} ((\beta_k^h)_{ij11})^* M_k^h \right) \bar{\epsilon_{11}} \tag{6.8}$$

Accordingly, the constraints on microstructure function in the DFT space transform to

$$\sum_{h=1}^{H} M_0^h = |\mathbf{S}|, \quad \sum_{h=1}^{H} M_{k\neq 0}^k = 0 \tag{6.9}$$

Then, replacing Eq.(7.3) into Eq.(7.2) we get

$$(e_{ij})_{k\neq 0} = \left(\sum_{h=1}^{2} (\beta_k^h)_{ij11}^* M_k^h \right) \bar{\epsilon}_{11} = (\beta_k^1 - \beta_k^2) * M_k^1 \bar{\epsilon}_{11} = \gamma_k^1 M_k^1 \bar{\epsilon}_{11} \tag{6.10}$$

$$(e_{ij})_0 = \left[(\beta_0^1 - \beta_0^2)^* M_0^1 + (\beta_0^2)^* |\mathbf{S}| \right] \bar{\epsilon}_{11} \tag{6.11}$$

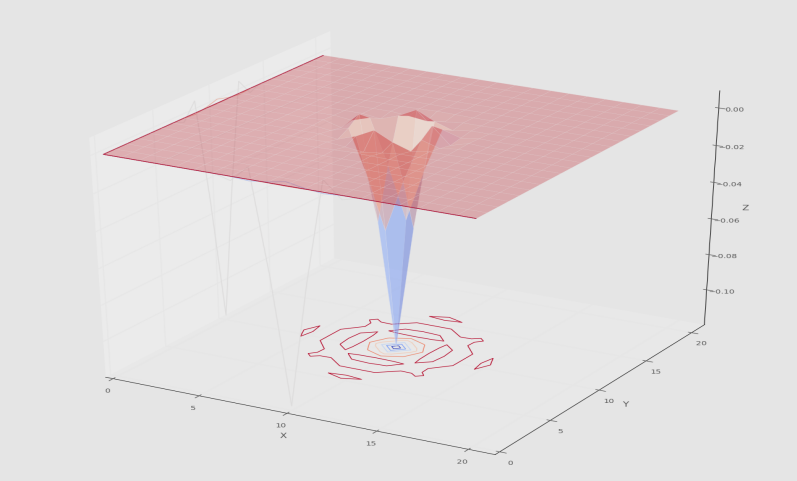

Figure 6.6: Visualization of influence function. It can be seen that the function dies out with increasing value of $\mathbf{t}$.

From the FE models, we obtain two datasets of $((e_{ij})_k, M_k^1)$. Next estimates of $(\gamma_k^1)_{ij11}$ which will best fit the datasets is found using linear regression analysis methods. As was mentioned

earlier, the influence coefficients are independent of each other, therefore only the values of γ_k^1. So, from the best estimates of $(\gamma_k^1)_{ij11}$ the values of $(\tilde{\alpha}_t^1)_{ij11} = \alpha_t^1)_{ij11} - \alpha_t^2)_{ij11}$ can be recovered. The function $\alpha_t^1)_{ij11}$ decays rapidly with increasing value of $\mathbf{t}$, which can be seen from Fig.(7.4).

Results and discussion

The coefficients of influence that were learnt from the FE analysis were used to predict the local response fields on application of a macroscale strain on a *random microstructure*. As can be seen the results obtained from both the procedures are in excellent agreement. However, the biggest advantage with using MKS is the saving of computational time. The MKS approach found the solution in 0.0039 sec whereas Abaqus took a CPU time of 21.30 secs both on a 8GHz CPU with 8GB RAM.

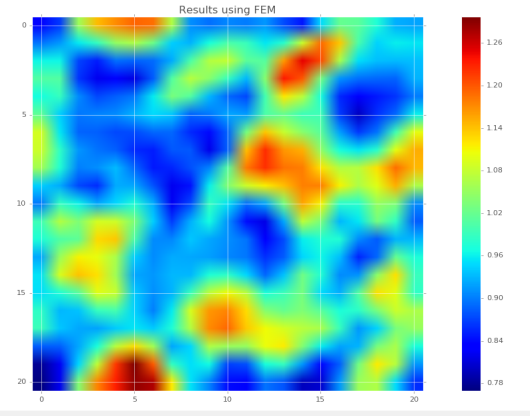

Figure 6.7: Predicted values of ϵ_{11} from the middle section of the random microstructure using FEM.

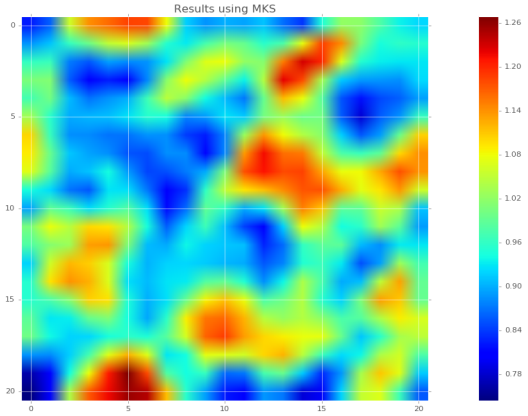

Figure 6.8: Predicted values of ϵ_{11} from the middle section of the random microstructure using MKS.

The error between DFT-based localization relationships and Finite Element methods can be given by

$$Err = \max_{s \in S} \left(\frac{((\epsilon_s)_{11})_{FEM} - ((\epsilon_s)_{11})_{MKS}}{\tilde{\epsilon}_{11}} \right) \text{x}100\% \tag{6.12}$$

The error between both methods was approximately 1%, as can be seen from the Fig.(7.7).

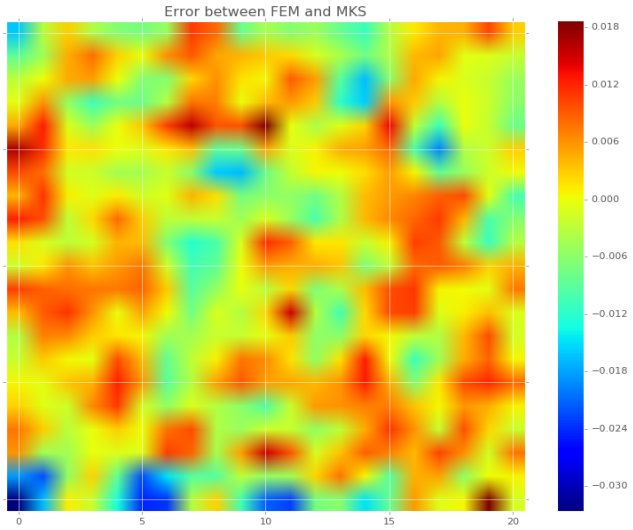

Figure 6.9: Periodic boundary conditions are applied using conditions described in Eq.(7.1).

References

[1] Hamad F Al-Harbi, Giacomo Landi, and Surya R Kalidindi. Multi-scale modeling of the elastic response of a structural component made from a composite material using the materials knowledge system. *Modelling and Simulation in Materials Science and Engineering*, 20(5):055001, 2012.

[2] Ahmet Cecen, Tony Fast, and Surya R Kalidindi. Versatile algorithms for the computation of 2-point spatial correlations in quantifying material structure. *Integrating Materials and Manufacturing Innovation*, 5(1):1, 2016.

[3] Anthony Nathan Fast. *Developing Higher-Order Materials Knowledge Systems*. PhD thesis, Drexel University, 2011.

[4] Hibbett, Karlsson, and Sorensen. *ABAQUS/standard: User's Manual*, volume 1. Hibbitt, Karlsson & Sorensen, 1998.

[5] Surya R Kalidindi. Data science and cyberinfrastructure: critical enablers for accelerated development of hierarchical materials. *International Materials Reviews*, 60(3):150–168, 2015.

[6] Surya R. Kalidindi, Stephen R. Niezgoda, Giacomo Landi, Shraddha Vachhani, and Tony Fast. A novel framework for building materials knowledge systems. *CMC*, 17(2):103–125, 2010.

[7] Giacomo Landi. *A Novel Spectral Approach to Multi-Scale Modeling*. 2011.

[8] Giacomo Landi, Stephen R. Niezgoda, and Surya R. Kalidindi. Multi-scale modeling of elastic response of three-dimensional voxel-based microstructure datasets using novel dft-based knowledge systems. *Acta Materialia*, 58(7):2716–2725, 2010.

[9] Giacomo Landi, Stephen R Niezgoda, and Surya R Kalidindi. Multi-scale modeling of elastic response of three-dimensional voxel-based microstructure datasets using novel dft-based knowledge systems. *Acta Materialia*, 58(7):2716–2725, 2010.

Chapter 7

Conclusions and Future Work

1. **Validation of MKS framework** This work demonstrated that MKS framework can be efficiently used for prediction of localised strains using DFT based approach. The effective property was calculated as the sum of series whose terms are made up of structure morphology and structure independent influence coefficients.

2. **Reduction in Computational Effort compared to FEM** The biggest advantage of MKS over FEM is the reduction in computational effort, by calibrating the coefficients against FE results. The calibration of influence coefficients for larger microstructure datasets is computationally expensive, but this is a one time effort because the influence coefficients are independent of the microstructure morphology. Once the calibration is done, results can be obtained very rapidly for any new random microstructure sets of the same material system.

3. **MKS Framework is extendable to High Contrast Materials** The numerical example presented here was for medium contrast composite material system, using only first order coefficients. For high contrast systems, where the ratio of Young moduli of the phases is more than 1.5, we will need to use higher order influence coefficients. The influence coefficient functions have compact support and die out with the increasing distance between spatial cell with a certain local state and the spatial cell of interest. This aligns naturally with the physics of material structure.

4. **High accuracy** A major improvement was seen in the calculation of results using MKS, with an accuracy of within 1% of the results obtained from FEM

5. **Use of Delta Microstructures for Calibration** It was demonstrated that using only two "delta" microstructures, are sufficient for calibration of the influence coefficients instead of calibrating against hundreds of microstructure samples.

6. **Established Localization Linkages can be used in Scale-Bridging multi-scale modelling simulations.** These relationship can capture the most prominent features of the *structure-property* linkages across disparate length scales. In the work done by [1] FEM was used on the macro-scale and spectral methods were used for prediction on the lower length scales.

7. **The MKS framework is in perfect alignment with Microstructure Informatics** MKS sets ground for true material-by-design methodology. It uses classification techniques from Data Science which further establishes the ground work for new generation of material databases, where the information will not be limited to only effective properties.

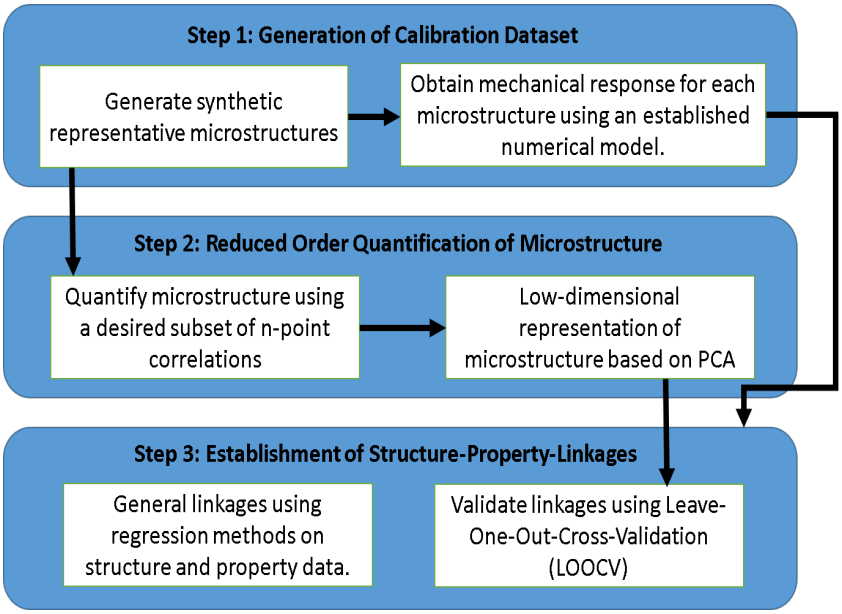

Figure 7.1: Main components of Data Science approach for establishing PSP linkages.

References

[1] Hamad F Al-Harbi, Giacomo Landi, and Surya R Kalidindi. Multi-scale modeling of the elastic response of a structural component made from a composite material using the materials knowledge system. *Modelling and Simulation in Materials Science and Engineering*, 20(5):055001, 2012.

Appendix A

Description of the code

In this section important functions of the code are commented.

```
#reads in the Abaqus output file and returns the desired strains for all
    elements in a 3d array
def ABstrains(ABout):
                f = open(ABout, 'r')
                cur_line = f.readline()
                while(cur_line != "" and "NUMBER OF ELEMENTS IS" not in
                    cur_line):
                        cur_line = f.readline()
                #get number of elements to loop through
                num_elements = int((cur_line.split())[4])
                currentStep = 1
                keepProcessing = True
                strains = None
                visco = False
                searchStaticOrVisco = "S T E P {} (S T A T I C A N A L Y S I
                    S)".format(currentStep)
                m = re.search(searchStaticOrVisco, cur_line)
                while(cur_line != "" and not m):
```

```
                cur_line = f.readline()
                m = re.search(searchStaticOrVisco, cur_line)
        if (cur_line == ""):
                return None
        if m.group(1) == "V I S C O A N A L Y S I S":
                visco = True
        while (keepProcessing):
                # Read strains for the next step, for static analysis,
                   there should be only one
                stepStrains = ReadStrainsStep(currentStep, f,
                   num_elements, visco)
                if (stepStrains == None):
                        keepProcessing = False
                else:
                        if strains == None:
                                strains = stepStrains
                        else:
                                strains = np.concatenate((strains,
                                   stepStrains), axis=3)
                currentStep = currentStep + 1
        return strains


#MicroSF are the Microstructure functions, ABout are the ABAQUS output file
   names, Macro is the imposed macro strain in the 11 direction
def GenC(MicroSF_1, MicroSF_2, ABout1, ABout2, Macro):
        #process ABAQUS output files and return 11 strains for each element
        strains_1 = ABstrains(ABout1)
        strains_2 = ABstrains(ABout2)
        strains_1 = strains_1/np.mean(strains_1)
```

```
strains_2 = strains_2/np.mean(strains_2)
#calculate DFT space responses and microstructure functions
response_1_k = np.fft.fftn(strains_1)
micro_1_k = zeros(MicroSF_1.shape,dtype=complex)
micro_1_k[:,:,:,0] = np.fft.fftn(MicroSF_1[:,:,:,0])
micro_1_k[:,:,:,1] = np.fft.fftn(MicroSF_1[:,:,:,1])
response_2_k = np.fft.fftn(strains_2)
micro_2_k = zeros(MicroSF_2.shape,dtype=complex)
micro_2_k[:,:,:,0] = np.fft.fftn(MicroSF_2[:,:,:,0])
micro_2_k[:,:,:,1] = np.fft.fftn(MicroSF_2[:,:,:,1])
#explicitly invert matrix and solve for coefficients
dim_len = response_1_k.shape[0]
coeff = zeros( (dim_len,dim_len,dim_len,2) , dtype=complex)
#attempt to perform least squares solution
for i in range(dim_len):
       for j in range(dim_len):
              for k in range(dim_len):
                     #u,v,w = i,j,k
                     #The following 2 quantities are used in the
                        normal equation during regression.
                     MM = np.zeros((2,2)) + 0j*np.zeros((2,2))#
                        Microstucture matrix (M' M*)
                     PM = np.zeros((2,1)) + 0j*np.zeros((2,1))#
                        Property matrix (P M*)
                     mSQc = np.conjugate(micro_1_k[i,j,k,:]) #
                        Conjugate of FFT of Microstructure
                     mSQt = np.mat(micro_1_k[i,j,k,:]).T # Transpose
                        of FFT of Microstructure
                     MM = MM + np.outer(mSQt,mSQc) # Calculate MM
```

```
                        PM = PM + (response_1_k[i,j,k] * mSQc) #
                            Calculate PM
                        mSQc = np.conjugate(micro_2_k[i,j,k,:]) #
                            Conjugate of FFT of Microstructure
                        mSQt = np.mat(micro_2_k[i,j,k,:]).T # Transpose
                            of FFT of Microstructure
                        MM = MM + np.outer(mSQt,mSQc) # Calculate MM
                        PM = PM + (response_2_k[i,j,k] * mSQc) #
                            Calculate PM
                        if ((i==0 and j ==0) and (k==0 or k==1)):
                            p = independent_columns(MM, .001)
                        calred = MM[p,:][:,p] # Linearly independent
                            columns of MM
                        resred = PM[p,0].conj().T # Linearly independent
                            columns of PM
                        coeff[i,j,k,p] = np.linalg.solve(calred, resred)
    #coeff[:,:,:] = response_1_k/micro_1_k[:,:,:,0]
    return coeff

#solves for new response given inputs
#macro is the imposed macro strain, coeff are the conj DFT coefficients,
   MSf is the microstructure function
#returns the spatial (not DFT) response
def NewResponse(coeff, macro, MSf):
    print np.nonzero(MSf)
    response = zeros(coeff.shape[0:3])
    MSf_DFT = zeros(MSf.shape,dtype=complex)
    MSf_DFT[:,:,:,0] = np.fft.fftn(MSf[:,:,:,0])
    MSf_DFT[:,:,:,1] = np.fft.fftn(MSf[:,:,:,1])
```

```
        response = lin_sum = np.sum(np.conjugate(coeff) * MSf_DFT[:,:,:,:], 3)
        response = np.fft.ifftn(response)
        return np.real_if_close(response)

This function takes an Eigen microstructure and returns a function that is
microstructure function in the fifth dimension of the array.
(The first four dimension will be used for space and time.)
The microstructure function provides the percentage of a voxel that belongs
to each state space.
For example

Input:
Eigen Microstructure
        [[1,2,1]
 MAT = [1,2,1]
         [1,2,2]]
Output:
Microstructure Function
        [[[[[1, 0]]] <- MAT[0,0] = 1
          [[[0, 1]]] <- MAT[0,1] = 2
          [[[1, 0]]]] <- MAT[0,2] = 1
         [[[[1, 0]]] <- MAT[1,0] = 1
MicroSF = [[[0, 1]]] <- MAT[1,1] = 2
          [[[1, 0]]]] <- MAT[1,2] = 1
         [[[[1, 0]]] <- MAT[2,0] = 1
          [[[0, 1]]] <- MAT[2,1] = 2
          [[[0, 1]]]]] <- MAT[2,2] = 2
'''
def MSf(MAT):
```

```
Dim = MAT.shape #np array dimension
l = len(Dim)
print "array dimensions = ",l
phases = sp.unique(MAT) #identify phases
print "unique phases = ",phases
numPhases = len(phases) #number of phases
print "number of phases = ", numPhases
if l == 2:
    MicroSF = np.zeros([Dim[0],Dim[1],1,1,numPhases])
    for ii in range(numPhases):
        Mask = np.ma.masked_equal(MAT, phases[ii])
        MicroSF[:,:,0,0,ii] = Mask*MicroSF[:,:,0,0,ii]
        MicroSF[:,:,0,0,ii] = MicroSF[:,:,0,0,ii]/phases[ii]
elif l == 3:
    MicroSF = np.zeros([Dim[0],Dim[1],Dim[2],1,numPhases])
    for ii in range(numPhases):
        Mask = np.ma.masked_equal(MAT, phases[ii])
        MicroSF[:,:,:,0,ii] = Mask*MicroSF[:,:,:,0,ii]
        MicroSF[:,:,:,0,ii] = MicroSF[:,:,:,0,ii]/phases[ii]
return MicroSF
```

```
This is the input file used to create the delta microstructure FE Model
    *Preprint, echo=NO, model=No, history=NO, contact=NO
*Heading
**************************************************
*node
1, 0, 0, 0
463, 0, 0, 20
22, 0, 20, 0
484, 0, 20, 20
10165, 20, 0, 0
10627, 20, 0, 20
10186, 20, 20, 0
10648, 20, 20, 20
**************************************************
*NSET, NSET=A
 1
*NSET, NSET=B
 463
*NSET, NSET=C
 22
*NSET, NSET=D
 484
*NSET, NSET=E
 10165
*NSET, NSET=F
 10627
*NSET, NSET=G
```

```
 10186
*NSET, NSET=H
 10648
**************************************************
*Nfill, Nset=AB
A, B, 21, 22
*Nfill, Nset=CD
C, D, 21, 22
*Nfill, Nset=ABCD
AB, CD, 21, 1
*Nfill, Nset=EF
E, F, 21, 22
*Nfill, Nset=GH
G, H, 21, 22
*Nfill, Nset=EFGH
EF, GH, 21, 1
*Nfill, Nset=ABCDEFGH
ABCD, EFGH, 21, 484
**************************************************
*Nfill, Nset=BD
B, D, 21, 1
*Nfill, Nset=FH
F, H, 21, 1
*Nfill, Nset=BDFH
BD, FH, 21, 484
**************************************************
** Bottom Face Node Set
*Nfill, Nset=AC
A, C, 21, 1
```

```
*Nfill, Nset=EG
E, G, 21, 1
*Nfill, Nset=ACEG
AC, EG, 21, 484
**************************************************
*ELEMENT, TYPE=C3D8
1,1,2,24,23,485,486,508,507
**************************************************
*ELGEN, elset=allel
1,21,1,1,21,22,21,21,484,441
**************************************************
*ELSET, ELSET=elset1
4631,
**************************************************
*ELSET, ELSET=elset2
1,   2,   3,   4,   5,   6,   7,   8,   9,   10,   11,   12,   13,   14,   15,   16,
17,   18,   19,   20,   21,   22,   23,   24,   25,   26,   27,   28,   29,   30,   31,
33,   34,   35,   36,   37,   38,   39,   40,   41,   42,   43,   44,   45,   46,   47,
49,   50,   51,   52,   53,   54,   55,   56,   57,   58,   59,   60,   61,   62,   63,
65,   66,   67,   68,   69,   70,   71,   72,   73,   74,   75,   76,   77,   78,   79,

.
.
.
.
NODE LIST HAS BEEN DELETED TO SAVE SPACE
.
.
.
```

```
**************************************************
*NSET, NSET=n3minus_n1minus
2,  3,  4,  5,  6,  7,  8,  9,  10,  11,  12,  13,  14,  15,  16,  17,
18,  19,  20,  21,
**************************************************
*NSET, NSET=n3minus_n1plus
10166,  10167,  10168,  10169,  10170,  10171,  10172,  10173,  10174,  10175,
10182,  10183,  10184,  10185,
**************************************************
*NSET, NSET=n2minus_n3minus
485,  969,  1453,  1937,  2421,  2905,  3389,  3873,  4357,  4841,  5325,  58
8229,  8713,  9197,  9681,
**************************************************
*NSET, NSET=n2plus_n3minus
506,  990,  1474,  1958,  2442,  2926,  3410,  3894,  4378,  4862,  5346,  58
8250,  8734,  9218,  9702,
**************************************************
*NSET, NSET=n3plus_n1minus
464,  465,  466,  467,  468,  469,  470,  471,  472,  473,  474,  475,  476,
480,  481,  482,  483,
**************************************************
*NSET, NSET=n3plus_n1plus
10628,  10629,  10630,  10631,  10632,  10633,  10634,  10635,  10636,  10637,
10644,  10645,  10646,  10647,
**************************************************
*NSET, NSET=n2minus_n3plus
947,  1431,  1915,  2399,  2883,  3367,  3851,  4335,  4819,  5303,  5787,  6
8691,  9175,  9659,  10143,
**************************************************
```

```
*NSET, NSET=n2plus_n3plus
968,  1452,  1936,  2420,  2904,  3388,  3872,  4356,  4840,  5324,  5808,  6
8712,  9196,  9680,  10164,
**************************************************
*NSET, NSET=n1plus_n2minus
10187,  10209,  10231,  10253,  10275,  10297,  10319,  10341,  10363,  10385,
10539,  10561,  10583,  10605,
**************************************************
*NSET, NSET=n1plus_n2plus
10208,  10230,  10252,  10274,  10296,  10318,  10340,  10362,  10384,  10406,
10560,  10582,  10604,  10626,
**************************************************
*NSET, NSET=n1minus_n2minus
23,  45,  67,  89,  111,  133,  155,  177,  199,  221,  243,  265,  287,  3
375,  397,  419,  441,
**************************************************
*NSET, NSET=n1minus_n2plus
44,  66,  88,  110,  132,  154,  176,  198,  220,  242,  264,  286,  308,
396,  418,  440,  462,
**************************************************
** Implement Periodic Boundary Conditions
*Equation
3
n1plus, 1, 1, n1minus, 1, -1, 10648, 1, -1
2
n1plus, 2, 1, n1minus, 2, -1
2
n1plus, 3, 1, n1minus, 3, -1
**
```

```
2
n2plus, 1, 1, n2minus, 1, -1
2
n2plus, 2, 1, n2minus, 2, -1
2
n2plus, 3, 1, n2minus, 3, -1
**
2
n3plus, 1, 1, n3minus, 1, -1
2
n3plus, 2, 1, n3minus, 2, -1
2
n3plus, 3, 1, n3minus, 3, -1
**
3
n1plus_n2plus, 1, 1, n1minus_n2plus, 1, -1, 10648, 1, -1
3
n1plus_n2minus, 1, 1, n1minus_n2minus, 1, -1, 10648, 1, -1
2
n1minus_n2plus, 1, 1, n1minus_n2minus, 1, -1
**
2
n1plus_n2plus, 2, 1, n1minus_n2plus, 2, -1
2
n1plus_n2minus, 2, 1, n1minus_n2minus, 2, -1
2
n1minus_n2plus, 2, 1, n1minus_n2minus, 2, -1
**
2
```

```
n1plus_n2plus, 3, 1, n1minus_n2plus, 3, -1
2
n1plus_n2minus, 3, 1, n1minus_n2minus, 3, -1
2
n1minus_n2plus, 3, 1, n1minus_n2minus, 3, -1
**
**
3
n3plus_n1plus, 1, 1, n3plus_n1minus, 1, -1, 10648, 1, -1
3
n3minus_n1plus, 1, 1, n3minus_n1minus, 1, -1, 10648, 1, -1
2
n3plus_n1minus, 1, 1, n3minus_n1minus, 1, -1
**
2
n3plus_n1plus, 2, 1, n3plus_n1minus, 2, -1
2
n3minus_n1plus, 2, 1, n3minus_n1minus, 2, -1
2
n3plus_n1minus, 2, 1, n3minus_n1minus, 2, -1
**
2
n3plus_n1plus, 3, 1, n3plus_n1minus, 3, -1
2
n3minus_n1plus, 3, 1, n3minus_n1minus, 3, -1
2
n3plus_n1minus, 3, 1, n3minus_n1minus, 3, -1
**
**
```

```
2
n2plus_n3plus, 1, 1, n2minus_n3plus, 1, -1
2
n2plus_n3minus, 1, 1, n2minus_n3minus, 1, -1
2
n2minus_n3plus, 1, 1, n2minus_n3minus, 1, -1
**
2
n2plus_n3plus, 2, 1, n2minus_n3plus, 2, -1
2
n2plus_n3minus, 2, 1, n2minus_n3minus, 2, -1
2
n2minus_n3plus, 2, 1, n2minus_n3minus, 2, -1
**
2
n2plus_n3plus, 3, 1, n2minus_n3plus, 3, -1
2
n2plus_n3minus, 3, 1, n2minus_n3minus, 3, -1
2
n2minus_n3plus, 3, 1, n2minus_n3minus, 3, -1
**** -------------------------------------------------------------
** MATERIALS
**
*Solid Section, elset=elset1, material=material-1
1.,
*Material, name=material-1
*Elastic,type=isotropic
120, 0.3
** Solid (element 2 = elset2)
```

```
**
*Solid Section, elset=elset2, material=material-2
1.,
**
*Material, name=material-2
*Elastic,type=isotropic
80, 0.3
** ----------------------------------------------------------------
**
** ----------------------------------------------------------------
**
** STEP: Step-1
**
*Step, name=Step-1
*Static
1., 1., 1e-05, 1.
**
** BOUNDARY CONDITIONS
**
** Name: BC-1 Type: Displacement/Rotation
*Boundary
**
1,1,3,0
463,1,3,0
22,1,3,0
484,1,3,0
10165,1,1,0.02
10627,1,1,0.02
10186,1,1,0.02
```

```
10648,1,1,0.02
10165,2,3,0
10627,2,3,0
10186,2,3,0
10648,2,3,0
**
** OUTPUT REQUESTS
**
*output, field, frequency=0
**
*output, history, frequency=0
**
*el print, summary=no, totals=yes
E
**
*End Step
```